PERGAMON

Journal of Quantitative Spectroscopy &
Radiative Transfer ▮▮▮ (▮▮▮▮) ▮▮▮–▮▮▮

Journal of
Quantitative
Spectroscopy &
Radiative
Transfer

www.elsevier.com/locate/jqsrt

Collisional parameters of H_2O lines: effects of vibration

Robert R. Gamache[a,*], Jean-Michel Hartmann[b]

[a] *Department of Environmental, Earth, and Atmospheric Sciences, University of Massachusetts Lowell,*
265 Riverside Street, Lowell, MA 01854, USA
[b] *Laboratoire de Photophysique Moléculaire, CNRS (UPR3361) et Université Paris-sud (bât. 350),*
91405 Orsay Cedex, France

Received 22 July 2002; accepted 29 October 2002

Abstract

A complex semiclassical model for the calculation of line widths and shifts of H_2O broadened by N_2, derived from the Robert and Bonamy approach, is tested by comparisons with measurements for selected transitions in various vibrational bands. The lines retained, which involve rotational states with $Kc = J$ or $J - 1$ have been chosen for two reasons. The first is that they show large variations of the widths with J and thus enable a severe test of the model. The second is that, as explained in this paper, they are well-suited for the study of the effects of vibration on the collisional parameters. The measured values have been extracted from an updated version of a database built years ago (JQSRT 52 (1994) 481) that contains all available measurements. Comparisons between experimental and calculated widths and shifts at room temperature illustrate the quality of the model and clearly demonstrate, for the first time, that there is a vibrational dependence of the broadening. Values of collisional parameters are first studied in fundamental bands. This shows that the theoretical approach accounts for most of the dependence of broadening and shifting on rotational quantum numbers: the variations of γ, which reach a factor of nearly 20 from low to high J values, are correctly accounted for by the model as are some specific features of the shifts δ. Analysis confirms that the bending and stretching vibrations have significantly different effects on δ, due to the vibrational dependence of the intermolecular potential. On the other hand, differences on the widths are rather small with slightly smaller broadening for lines of the bending band. Calculations show that there is a spectroscopic effect, due to the larger rotational constant A in the $v_2 = 1$ state. Calculations made for overtone bands involving numerous quanta of the stretching vibration are then presented. They predict that a significant dependence of the width should be observed for high J lines due to the effect of vibration on the interaction potential. This is confirmed by comparisons with measurements for lines involving a change of three and four quanta of stretching vibration.

---

[*] Corresponding author. Tel.: +1-978-934-3904; fax: +1-978-934-3069.
E-mail address: robert_gamache@uml.edu (R.R. Gamache).

0022-4073/02/$ - see front matter © 2002 Published by Elsevier Science Ltd.
PII: S0022-4073(02)00296-0

1. Introduction

The shape of well-isolated spectral lines at moderate pressures is often described in terms of the pressure-broadened half-width, γ, and the pressure induced line shift, δ, of a Lorentz profile. These parameters arise due to collisions between the active (radiating) molecule and those of the bath (perturber). Both γ and δ are expressed in terms of the intermolecular potential between the radiating and perturbing molecules. For infrared transitions, this potential can be thought of as components which depend on the vibrational and rotational states involved in the considered optical transition. It is important to realize that the half-width and line shift are functions of both the real and imaginary parts of vibration and rotation terms.

The collision process takes the radiating molecule from a rotational state i to i' and the perturbing molecule from rotational state J_2 to J_2'. When the energy gaps from $i \rightarrow i'$ and $J_2 \rightarrow J_2'$ match, $\Delta E_{i,i'} = -\Delta E_{J_2,J_2'}$, the process is said to be resonant. Whereas the half-width is dominated by the real part of the rotational part of the potential when the collisions are resonant, the shifts are sensitive to both the rotational and vibrational parts. However, as the difference in energy gaps increases the collisions are off resonance and less and less efficient in inducing rotational changes; the vibrational terms can then contribute significantly to both the half-width and shift. For certain transitions that are well off resonance these parameters are due almost entirely to the vibrational part of the potential and are then practically constant and insensitive to the rotational states. An example of this effect is observed with the lighter hydrogen halides, HF and HCl, which have a large vibrational anharmonicity and have rotational constants B of roughly 20 and 10 cm^{-1}, respectively. For HF in the ground vibrational state, the half-width approaches zero (no vibrational contribution) by about $J''=7$ or 8 [1,2] and for HCl this requires a J'' value of 15–16 [3]. Indeed, the associated rotational changes involve large energy jumps ($\sim 300\ \mathrm{cm}^{-1}$ for $|\Delta J| = 1$ and much more for $|\Delta J| = 2, 3, \ldots$) and are poorly induced by collisions at room temperature. For HF transitions in the 1-0 and 2-0 bands the half-widths approach constant values of about 0.006 and 0.020 cm^{-1}/atm whereas the shifts tend to -0.03 and $-0.05\ \mathrm{cm}^{-1}$/atm, which are due only to the vibrational contribution [1,2]. In more complex molecules this effect is not so clear due to increased structure. For water vapor, a light asymmetric rotor, the transitions are labeled by upper and lower state rotational quantum number J and the pseudo-quantum numbers Ka and Kc. Transitions occur with many values of ΔJ, ΔKa, and ΔKc which complicate attempts to derive rules dependent on the rotational quantum number J or to examine the vibrational dependence of the collisional parameters.

The question of the influence of vibration on the half-widths of water vapor was addressed in a survey paper [4] and several workshops [5–7]. It was estimated that the effect of the vibrational states of the transition was smaller than experimental uncertainties and could change the half-width by no more than 3–5%. However, the suggestion that the half-widths of water vapor may be dependent on the vibrational states has been made in a number of papers [8–12]. Mandin et al. [8,9] in two studies dealing with the 8500–9300 and 9500–11500 cm^{-1} regions took ratios of their measured values to those of the HITRAN database [13]. From this they concluded that there was a small (±3%) vibrational dependence of the half-width. Grossman and Browell [10], using average broadening values, reported a 5% difference between transitions in the $3v_1 + v_3$ and $2v_1 + 2v_2 + v_3$ bands with the $3v_1 + v_3$ lines having the larger broadening values. In a 1996 study by Brown and Plymate [11] on H_2O broadened by hydrogen, the ratios of half-widths for the same set of rotational quantum numbers were formed for the rotation and ν_1 bands divided by the ν_2 band, 51 and 63 pairs of transitions, respectively. The ratios of the rotation to the ν_2 band range from 0.92 to 1.1 and those of the ν_1 to ν_2 band range from 0.98 to 1.19 for the transitions studied. For rotational/ν_2 transitions the rms ratio is 1.016 (±2.6%) and 1.08 (±4%) for ν_1/ν_2. Brown and Plymate concluded that these differences are too large to be caused by experimental error and that there is a vibrational dependence in the half-width. A 2002 study by Zou and Varanasi [12] of self- and air-broadening and shifting of water vapor in the 950–2100 and 3000–4050 cm^{-1} regions also looked into the vibrational dependence of the half-width. Ratios of the half-widths for the same rotational transition were formed for the $2\nu_2$ and the ν_2 bands, the ν_1 and the ν_2 bands, and the $2\nu_2$ and the ν_1 bands for both self- and air-broadening. From the analysis of the self-broadening data they conclude that the half-widths in the $2\nu_2$ band are smaller than their counterparts in the ν_2 band by about 10%. The differences in the ratios for the ν_1 and the ν_2 bands, and the $2\nu_2$ and the ν_1 bands contained too much scatter to state conclusively if there was any vibrational dependence. The analysis of the air-broadening data indicated that the half-widths in the ν_1 band are larger than the corresponding half-widths in the ν_2 band by about 5%. This is in rough agreement with the work of Brown and Plymate [11]. There were too few ratios for the $2\nu_2$ and the ν_2 bands and the $2\nu_2$ and the ν_1 bands to draw any solid conclusions about the vibrational dependence of the half-widths.

The vibrational dependence of the half-width arises from two factors: one designated a spectroscopic effect and another which is purely a vibrational effect. The first results from the fact that a change in the vibrational state also leads to slightly different rotational wave functions, energy gaps, and transition probabilities between the rotational internal states. The second is that a change of vibrational state in a transition leads to changes in the half-width due to the difference in the vibrational part of the intermolecular potential. Lynch et al. [14] and Gamache et al. [15] have discussed, from the point of view of the theory, the importance of the vibrational dephasing terms resulting from the dependence of the isotropic intermolecular interaction on the vibrational state. For transitions where this term is dominant a strong vibrational dependence of the half-width should be expected. Both studies emphasized that the final value determined for the half-width comes from an interplay of many terms in the potential which have an importance that varies as the internuclear separation changes. These facts make it difficult to associate the final half-width with any single term in the potential or in the expressions for the half-width. Furthermore, in the earlier studies the uncertainties on the half-widths coupled with a relatively small number of data and the lack of measurement for certain types of transitions made it difficult to detect any strong dependence of the half-width on vibration. The studies on HF and HCl indicate that transitions where the energy gap between collisionally coupled levels is large and that have very small broadening values in the ground vibrational state are good candidates to demonstrate the effects of vibration. For water vapor the energy gap for most collision induced transitions seldom exceeds 100 cm^{-1}. However, for the lines involving levels with $Kc = J$ (or $J - 1$) the energy gaps increase quickly with J and the half-width decreases by a factor of ~ 20 from $J'' = 0$ to 18, a behavior similar to the light hydrogen halides.

In this paper the measured half-widths and line shifts of the $Kc = J - 1$ and J doublet transitions of water broadened by nitrogen for a number of vibrational transitions are studied and compared with theoretical predictions made employing the complex Robert–Bonamy (CRB) formalism [15]. The experimental data is extracted from a database where all available measurements have been included. The calculations explore a number of changes in vibrational quanta for doublets up to $J'' = 18$. Comparisons between experimental and calculated values for the half-widths and shifts of lines of the fundamental bands are first made. They demonstrate the quality of the CRB approach and validate the data used. Analysis shows that (small) differences exist between widths of the ν_2 and ν_1 band, for instance, that are essentially due to differences in the rotational energy structure of the $v_2 = 1$ and $v_1 = 1$ levels. A study of line-broadening for overtone transitions is then made. It is shown that a significant and increasing effect of the vibrational state can be observed and predicted for high J lines of bands involving numerous quanta of the stretching modes. Differences between the widths of such lines and those of similar transitions in the fundamentals are shown to arise from the vibrational dependence of the interaction potential between the H_2O molecule and the collision partner.

2. Complex Robert–Bonamy formalism

A full description of the complex Robert–Bonamy formalism can be found in Refs. [15–17], here only the salient features are given. The formalism is based on the resolvent operator formalism of Baranger [18], Kolb [19], and Greim [20] (BKG) and is complex valued so that the half-width and line shift are obtained from a single calculation. The application of linked-cluster techniques [21] to the BKG formalism yields developments [22–25] which eliminate the awkward cutoff procedure that characterized earlier theories [26–28]. The intermolecular dynamics are treated more realistically than in the earlier approaches, i.e. using curved rather than straight line trajectories. This has important consequences in the description of close intermolecular collisions (small impact parameters). Also important for close collision systems is the incorporation in the CRB theory [22] of a short range (Lennard–Jones 6–12 [29]) atom–atom component to the intermolecular potential. This component has been shown to be essential for a proper description of pressure broadening, especially in systems where electrostatic interactions are weak [30]. (Here, the notion of strong and weak collisions adopts the definition of Oka [31]).

The half-width, γ, and line shift, δ, of a ro-vibrational transition $f \leftarrow i$ are given in the complex Robert–Bonamy (CRB) formalism by minus the imaginary part and the real part, respectively, of the diagonal elements of the complex relaxation matrix. In computational form used here, the half-width and line shift are usually expressed in terms of the scattering matrix [18,32]

$$(\gamma + \mathrm{i}\delta)_{f\leftarrow i} = \frac{n_2}{2\pi c}\langle v \times [1 - \mathrm{e}^{-{}^{R}S_2(f,i,J_2,v,b)}\mathrm{e}^{-\mathrm{i}[S_1(f,i,J_2,v,b)+{}^{I}S_2(f,i,J_2,v,b)]}]\rangle_{v,b,J_2}, \qquad (1)$$

where n_2 is the number density of perturbers and $\langle\cdots\rangle_{v,b,J_2}$ represents an average over all trajectories (impact parameter b and initial relative velocity v) and initial rotational state J_2 of the collision partner. S_1 (real) and $S_2 = {}^{R}S_2 + i\,{}^{I}S_2$ are the first and second order terms in the expansion of the scattering matrix; they depend on the rovibrational states involved and associated collision-induced jumps from these levels, on the intermolecular potential and characteristics of the collision dynamics. The exact forms of the S_2 and S_1 terms are given in Refs. [15–17].

The S_1 term, which makes a purely imaginary contribution, is isotropic in the absence of any vibrational dependence of the anisotropic intermolecular forces. It then has the appellation of the vibrational dephasing term and arises only for transitions where there is a change in the vibrational state. The potential leading to S_1 is written in terms of the isotropic induction and London dispersion interactions:

$$V_{\text{iso}}^{\text{induction}} = -\frac{\mu_1^2\alpha_2}{R^6},$$

$$V_{\text{iso}}^{\text{dispersion}} = -\frac{3}{2}\frac{I_1 I_2}{I_1+I_2}\frac{\alpha_1\alpha_2}{R^6}, \tag{2}$$

where μ_1 is the dipole moment of water vapor and α_k and I_k are the polarizability and ionization potential for water vapor ($k=1$) and collision partner ($k=2$). The vibrational dependence of these terms is contained in the dipole moment, μ_1, and polarizability, α_1, of water vapor. The first was investigated by Shostak and Muenter [33] and is given in Debyes by

$$\mu = 1.855 + 0.0051\left(v_1+\frac{1}{2}\right) - 0.0317\left(v_2+\frac{1}{2}\right) + 0.0225\left(v_3+\frac{1}{2}\right), \tag{3}$$

where v_n is the number of quanta in the nth normal mode. The polarizability of water vapor was obtained by Luo et al. [34] and is, in atomic units [35] [1]

$$\alpha = 9.86 + 0.29\left(v_1+\frac{1}{2}\right) + 0.03\left(v_2+\frac{1}{2}\right) + 0.28\left(v_3+\frac{1}{2}\right). \tag{4}$$

The $S_2 = {}^RS_2 + i\,{}^IS_2$ term is complex valued and results from the anisotropic interactions. The potential employed in the calculations consists of the leading electrostatic components for the H_2O–X pair (the dipole and quadrupole moments of H_2O with the quadrupole moment of N_2) and atom–atom interactions [15,36]. The latter are defined as the sum of pair-wise Lennard–Jones 6–12 interactions [29] between atoms of the radiating (1) and the perturbing (2) molecules,

$$V^{\text{at—at}} = \sum_{i=1}^{n}\sum_{j=1}^{m} 4\varepsilon_{ij}\left\{\frac{\sigma_{ij}^{12}}{r_{1i,2j}^{12}} - \frac{\sigma_{ij}^{6}}{r_{1i,2j}^{6}}\right\}. \tag{5}$$

The subscripts $1i$ and $2j$ refer to the ith atom of molecule 1 and the jth atom of molecule 2, respectively, n and m are the number of atoms in molecules 1 and 2, respectively, and ε_{ij} and σ_{ij} are the Lennard–Jones parameters for the atomic pairs. The heteronuclear atom–atom parameters can be constructed from homonuclear atom–atom parameters (ε_i and σ_i) by the "combination rules" of Hirschfelder et al. [37] or Good and Hope [38]. The atom–atom distance, r_{ij} is expressed in terms of the center of mass separation, R, via the expansion in $1/R$ of Sack [39]. This development being truncated, sufficient order must be chosen to insure the convergence of calculated half-widths and line shifts, as has been discussed by Labani et al. [40] and by Gamache et al. [14,16,36]. Here the formulation of Neshyba and Gamache [36] expanded to eighth order is used.

Finally, recall that the isotropic component of the atom–atom potential is used to define the trajectory of the collisions within the semiclassical model of Robert and Bonamy [22].

---

[1] The choice of units for Eqs. (3) and (4) is made to keep the expressions as concise as possible. For conversion to other units see for example [35].

3. Experimental and theoretical data

3.1. Measured values

With respect to the situation about 10 years ago [4], the number of experimental determinations of water vapor line broadening and shifting parameters has increased considerably [41]. For H_2O–N_2 and H_2O–air mixtures, which are considered in the present work, more than 60 references [8–10,12, 42–102] have been published in the last 30 years, providing more than ten thousand values of the widths and/or shifts. In many cases, a given transition has been measured by various authors (see example in Table 1 below) thus enabling inter-comparison of the measurements and the determination of reliable values of the considered parameter and of the associated uncertainty. In order to enlarge the available data set, we have considered both the H_2O–N_2 and H_2O–air systems. The data for air-broadening has been converted to nitrogen broadening by multiplying it by the value 1.09 as suggested in the HITRAN database [13]. This procedure, although approximate since γ_{N2}/γ_{air} varies from line to line, is expected to be precise within a few percent which is sufficient in view of the experimental uncertainties and the precision of the calculations as well as considering the purpose of the present work. For the line-shifts, we have assumed $\delta_{N2} = \delta_{air}$ which, again, is a rough approximation but sufficient. For any of the specific lines considered here (see below), an "experimental" value and associated uncertainty were determined using all available measurements (except, in some cases for some that are clearly away from all others). The retained value was simply computed as the average of available data and the uncertainty was obtained from the maximum difference between this average value and the measurements. Note that the default values of $\Delta\gamma = 5\%$ and $\Delta\delta = 10^{-3}$ cm^{-1}/atm, which seem reasonable in view of the scatter of measurements [4,41], were imposed in cases where calculated uncertainties were smaller.

3.2. Choice of the transitions

Besides the test of the model, the other aim of the present work is to study and to try to identify any vibrational dependence of the half-widths. In order to choose the best set of transitions to fulfill

Table 1
Experimental values of half-widths and shifts (in 10^{-3} cm^{-1}/atm) of some N_2 broadened $Kc = J$ and $J-1$ H_2O lines of the v_2 band. Underlined values have been deduced from H_2O–air measurements (see text)

$16_{0,16} \leftarrow 15_{1,15}$		$12_{2,11} \leftarrow 11_{1,10}$		$6_{1,6} \leftarrow 7_{0,7}$		$2_{1,2} \leftarrow 1_{0,1}$	
γ	δ	γ	δ	γ	δ	γ	δ
$\underline{7.52}$ [50]	$-\underline{4.25}$ [92]	$\underline{24.7}$ [92]	$-\underline{0.95}$ [92]	$\underline{63.2}$ [12]	$-\underline{1.80}$ [12]	$\underline{142}$ [57]	$+\underline{4.40}$ [92]
$\underline{8.18}$ [43]	$-\underline{4.48}$ [80]	$\underline{24.9}$ [46]	$-\underline{1.10}$ [12]	$\underline{64.0}$ [72]	$-\underline{1.85}$ [92]	$\underline{117}$ [72]	$+\underline{5.60}$ [12]
$\underline{7.63}$ [47]	$-\underline{3.80}$ [42]	$\underline{27.6}$ [51]	$-\underline{1.70}$ [80]	$\underline{64.8}$ [92]	−1.50 [92]	$\underline{108}$ [92]	+6.01 [92]
$\underline{7.30}$ [80]	−3.29 [42]	$\underline{24.2}$ [80]	−0.25 [92]	67.3 [72]		$\underline{111}$ [12]	
$\underline{7.85}$ [92]	−4.15 [90]	$\underline{23.5}$ [12]	−1.15 [90]	66.5 [92]		144 [57]	
7.60 [94]	−4.14 [92]	24.9 [92]				123 [72]	
7.20 [42]						117 [92]	
7.10 [47]							
8.00 [92]							

such purposes, let us consider, for instance, two lines with identical rotational quantum numbers belonging to the rotational band $(0f \leftarrow 0i)$ and to another vibrational transition starting from the ground state $(vf \leftarrow 0i)$. Starting from Eq. (1), with simplified notations, their widths and shifts can be written as

$$(\gamma + i\delta)_{0f\leftarrow 0i} = \langle 1 - \exp^{-{}^{R}S_2(0f,0i)}\{\cos[{}^{I}S_2(0f,0i)] - i\sin[{}^{I}S_2(0f,0i)]\}\rangle,$$

$$(\gamma + i\delta)_{vf\leftarrow 0i} = \langle 1 - \exp^{-{}^{R}S_2(vf,0i)}\{\cos[{}^{I}S_2(vf,0i) + S_1(v,0)] - i\sin[{}^{I}S_2(vf,0i) + S_1(v,0)]\}\rangle, \quad (6)$$

where we have accounted for the fact that S_1 is a purely vibrational term (hence $S_1(0,0) = 0$ since $\Delta v = 0$ for rotational lines), independent of rotational quantum numbers. Recall that the S_2 terms result from anisotropic interactions only which, in the present approach, are calculated using a potential that does not depend on vibration. Hence, differences between collisional parameters of the two lines (i.e., the vibrational dependence) arise from two main factors: The first is a spectroscopic effect associated with the fact that the energy structure and wave functions of the rotational levels are different in the 0 and v vibrational states. This induces differences in the S_2 terms, namely in both the real and imaginary parts of the $S_{2,\mathrm{outer}f}$ and $S_{2,\mathrm{middle}}$ contributions [15–17], through changes in the potential operator matrix elements and in the arguments of the resonance functions. The second effect is due to the vibrational dependence of the interaction potential which results in the nonzero value of $S_1(v,0)$. For further analysis, let us assume (which is true in practice), that ${}^{I}S_2$ and S_1 are small, as well as the difference ${}^{R}S_2(vf,0i) - {}^{R}S_2(0f,0i)$ so that linear developments can be made.

When the purely vibrational effects are negligible ($S_1 = 0$), the development keeping only the leading terms (assuming that $\cos(x)$ and $\sin(x)$ can be approximated to one and x, respectively) leads to

$$\gamma_{vf\leftarrow 0i} = \gamma_{0f\leftarrow 0i} + \langle \exp^{-{}^{R}S_2(0f,0i)} \times \{[{}^{R}S_2(vf,0i) - {}^{R}S_2(0f,0i)] + {}^{I}S_2(0f,0i)[{}^{I}S_2(vf,0i) - {}^{I}S_2(0f,0i)]\}\rangle,$$

$$\delta_{vf\leftarrow 0i} = \delta_{0f\leftarrow 0i} + \langle \exp^{-{}^{R}S_2(0f,0i)} \times \{[{}^{I}S_2(vf,0i) - {}^{I}S_2(0f,0i)] - {}^{I}S_2(0f,0i)[{}^{R}S_2(vf,0i) - {}^{R}S_2(0f,0i)]\}\rangle. \quad (7)$$

These show that dependences of the widths and shifts due to spectroscopic effects need significant changes in the real and imaginary parts of $S_{2,\mathrm{outer}f}$ and $S_{2,\mathrm{middle}}$ when going from the fundamental to the v vibrational level. These terms depend on reduced matrix elements and rotational energy gaps between level f and any other level f' to which f is collisionally connected. Changes in these terms from one vibrational state to another are small for the first rotational levels and generally strongly increase with the rotational energy (e.g. differences in the energy grids of the 000 and 010 induced by the different constants A). This analysis shows that lines involving levels of high rotational levels (high J and $|Ka - Kc|$) are the best candidates for the study of vibrational dependence through spectroscopic effects.

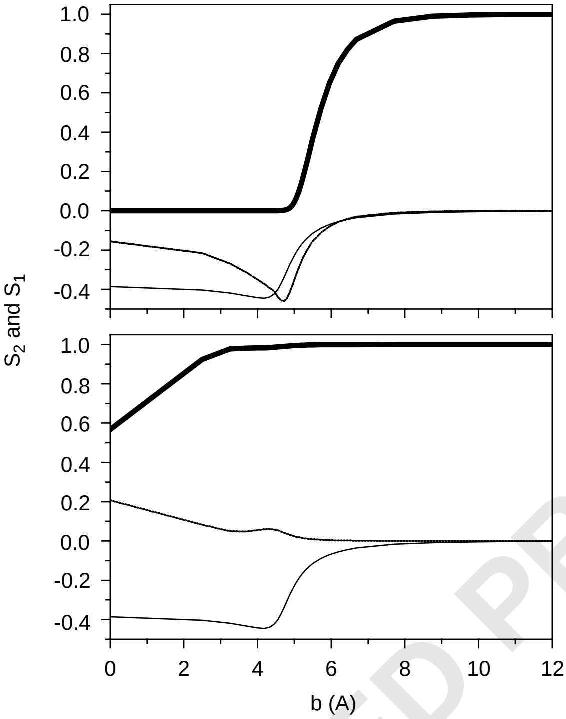

Fig. 1. Calculated values of exp(-$^RS_2$)(—), $^IS_2$ (- - -) and S_1 (—) versus the impact parameter b for a broad line (top panel) and a narrow line (lower panel).

If, on the contrary, the difference $S_2(vf,0i)-S_2(0f,0i)$, due to spectroscopic effects, is negligible, the effect of vibration, through S_1, is given by

$$\gamma_{vf\leftarrow 0i}=\gamma_{0f\leftarrow 0i}+\langle \exp[-{}^RS_2(0f,0i)]\times[S_1(v,0)^2/2+S_1(v,0)\times{}^IS_2(0f,0i)]\rangle,$$

$$\delta_{vf\leftarrow 0i}=\delta_{0f\leftarrow 0i}+\langle \exp[-{}^RS_2(0f,0i)]\times S_1(v,0)\rangle. \tag{8}$$

Typical variations of exp(-$^RS_2$), $^IS_2$, and S_1 with the impact parameter are plotted in Fig. 1 for a broad (low J) and a narrow (high J) line. In the case of transitions with large broadening parameters, exp(-$^RS_2$) is nearly zero over a significant range of impact parameters (up to about $b\approx\sqrt{(2c\gamma)/(n_2\bar{v})}$ where $\bar{v}$ is the mean relative velocity [103]) thus strongly masking the contribution of S_1 to both the width and shift. On the contrary, for narrow lines, exp(-$^RS_2$) is nearly one so that the vibrational dephasing term can make a significant contribution. Furthermore, note that Eqs. (2)–(4) result in a vibrational dependence of S_1 of the form

$$S_1[(v_1',v_2',v_3')\leftarrow(v_1'',v_2'',v_3'')]=c_1\Delta v_1+c_2\Delta v_2+c_3\Delta v_3, \tag{9}$$

where $\Delta v_i=v_i'-v_i''$ ($i=1$–3) is the variation of vibrational quanta of the ith mode for the considered transition. Analysis of the numerical values of the parameters of Eqs. (2)–(4) shows that S_1 is dominated by the contribution of dispersion forces so that c_1, c_2 and c_3 are mostly related to the numbers in Eq. (4). This indicates that significantly stronger vibrational effects can be expected from the excitation of the v_1 or v_3 modes than of the v_2 mode. Indeed, for high J lines with small values of ${}^{R}S_2(0f \leftarrow 0i)$ and ${}^{I}S_2(0f \leftarrow 0i)$ (and thus of $\gamma_{0f\leftarrow 0i}$] one would expect, from Eqs. (4), (8), and (9), the following dependences:[2]

$$\gamma_{\Delta v_1 \Delta v_2 \Delta v_3 f \leftarrow 0i} \propto [\Delta v_1 + \Delta v_2/10 + \Delta v_3]^2,$$

$$\delta_{\Delta v_1 \Delta v_2 \Delta v_3 f \leftarrow 0i} \propto [\Delta v_1 + \Delta v_2/10 + \Delta v_3]. \tag{10}$$

The conclusion of this preliminary study is that the best candidates for the study of vibrational effects on the widths (and the shifts) are lines involving levels of high rotational energies. These are likely those for which differences due to the spectroscopic structure of various vibrational states are the largest. Such transitions, in fundamental and high overtone bands with strong excitations of the stretching modes, are also suited for a study of the influence of the vibrational dependence of the potential through the S_1 contribution since they are very narrow. Furthermore, for a significant test of the semiclassical model, a representative set of transitions showing large, medium, and small values of the shifts and widths should be used. These considerations and the analysis of the available data has led us to the choice of transitions involving rotational states with $Kc = J$ or $J - 1$. These are doublets with two components associated with $Ka = J - Kc$ and $Ka = J - Kc + 1$. They have the advantage of having been relatively well-studied and of showing large and smooth variations of the N_2 broadening coefficients with J (typically from 0.11 cm^{-1}/atm for $1_{1,1} \leftarrow 2_{0,2}$ to 0.006 cm^{-1}/atm for $17_{1,17} \leftarrow 18_{0,18}$ in the v_2 band [92], also see Table 1)

3.3. Data and choices for the calculations

For water vapor, the reduced matrix elements are evaluated using wavefunctions determined by diagonalizing the Watson Hamiltonian [104] in a symmetric top basis for the vibrational states involved in the transition. For the ground state, the Watson constants of Matsushima et al. [105] were used. For the v_2, v_1, and v_3 bands the Watson constants derived by Flaud and Camy-Peyret [106] were used. For the $2v_1 + 2v_2 + v_3$ and $3v_1 + v_3$ bands the constants of Grossmann et al. [107] were used. The calculations were made at 296 K. In addition, calculations were made for the $(n00) \leftarrow (000)$ bands, with $n = 1, 2, 3, 4, 5, 6$, where the rotational state Watson constants were used because constants were not available for most of these bands. Note, this neglects the spectroscopic contribution to the half-width due to the change in vibrational state but such effects are small as will be shown later on. The rotational constant for N_2 is 2.0069 cm^{-1} [108].

Many of the molecular parameters for the H_2O–N_2 system are well known and the present calculations use the best available values from the literature. The dipole and quadrupole moments of water vapor are taken from Refs. [109,110], respectively. The quadrupole moment of nitrogen is from Mulder et al. [111]. The numerical values are listed in Table 2. The ionization potential of water is taken to be a vibrationally-independent value of 12.6 eV [112]. For nitrogen the polarizability, 17.4×10^{-25} cm^3, is taken from Ref. [113] and the ionization potential, 15.576 eV, from Ref. [114]. In the parabolic approximation, the isotropic part of the interaction potential is taken into account in

---

[2] Note that the value of 10 in this equation is obtained from the ab-initio values of Eq. (4). As explained in the next section, results indicate that the 0.03 value for the v_2 mode should be changed to 0.07. Hence $\Delta v_2/10$ should be then changed to about $\Delta v_2/4$.

Table 2
Values of electrostatic moments for the water vapor and nitrogen

Molecule	Multipole moment	Reference
H_2O	$\mu = 1.8549 \times 10^{-18}$ esu	[33]
	$Q_{xx} = -0.13 \times 10^{-26}$ esu	[110]
	$Q_{yy} = -2.5 \times 10^{-26}$ esu	[110]
	$Q_{zz} = 2.63 \times 10^{-26}$ esu	[110]
N_2	$Q_{zz} = -1.4 \times 10^{-26}$ esu	[111]

determining the distance, effective velocity, and force at closest approach [22]. To simplify the trajectory calculations, the isotropic part of the atom–atom expansion is fit to an isotropic Lennard–Jones 6–12. The atom–atom parameters have been determined by taking the homonuclear-atom–atom parameters obtained by Bouanich [115] and using the combination rules [37] to produce the heteronuclear atom–atom parameters.

Calculations made using these parameters for some transitions in the ν_2 band showed structured discrepancies when compared with measurements of both the shifts and widths. In a recent study of the lesser isotopomers of water vapor [116] it was observed that a relatively small change in the atom–atom parameters for the N–D and D–O interactions resulted in much improved agreement with measurement. Furthermore, there are a number of different methods which have been proposed to determine heteronuclear potential parameters from homonuclear parameters [117,118, (and references therein)]. Good and Hope [38] showed that different combination rules for ε lead to variations in ε of ~15%. Thus the resulting parameters have an increased uncertainty (besides that resulting from the imprecision of the homonuclear data) which depends on the method chosen to go from the homonuclear to the heteronuclear parameters. From these elements, we conclude that adjustment of the atom–atom parameters within ~15% around the values given by the combination formula of Hirchfelder et al. is not unreasonable provided there are reliable experimental data on collisional parameters for adjustment.

In order to improve the quality of calculations for nitrogen broadening of $H_2{}^{16}O$, six transitions of the ν_2 band were chosen for which there are multiple measurements and for which the calculated widths using unadjusted atom–atom parameters were too high for two lines, too low for two lines, and in agreement for the last two transitions. The potential parameters ε_{HN}, σ_{HN}, ε_{ON}, and σ_{ON} were adjusted to give a good fit of all these lines. With respect to the starting values (from combination rules of Ref. [37] and the homonuclear data by Bouanich [115]), the final parameters correspond to a 10% lowering of ε_{ON}, a 10% increase in ε_{HN}, a 3.9/in σ_{HN}, and no change in σ_{ON}.[3] The final adjustment of the potential parameters was made by comparing calculated line shifts to measurement. For transitions involving changes in the numbers of quanta in ν_1 and ν_3 the calculations made using the coefficients in Eq. (4) give sufficiently good agreement with the measurements (see results hereafter and Ref [16]). Comparing calculations for the ν_2 band with the measurements of Toth [92] indicated the ab-initio value of 0.03 in Eq. (4) should be changed to 0.07.

---

[3] Note, a full least-squares minimization was not thought worthwhile until the work of Ref. [41] and a detailed study of velocity averaging effects (see below) are completed.

In the present study, the widths have been calculated without performing the averaging over the Boltzmann distribution of velocities. Only the mean thermal value $\bar{v}$ was used as has been done in most previous calculations. This choice was made for the following reasons: the first is that performing the velocity averaging is costly and unnecessary for the purpose of the present study. Indeed, even though use of $\bar{v}$ may be approximate (errors being partially corrected by the use of adjusted potential parameters), it will lead to similar errors in the various bands for transitions with identical rotational quantum numbers. Hence analysis of the effects of the vibrational state on the widths and shifts with the present approach permits conclusive remarks. The second reason for our choice is the following: for some systems the dependence of the width on velocity is weak and calculations using only $\bar{v}$ lead to correct results. This is generally the case for H_2O lines at room temperature [119] and one can easily show that the $\bar{v}$ approximation is exact for lines for which $\gamma(v)$ is independent of v or proportional to v^1. On the other hand, if the dependence on v is strong the effect of the averaging will be significant but in this case the line shape will likely differ from a Lorentzian. Indeed, the proper shape would then be an average over the H_2O absolute velocity of a line shape in which collisional parameters are averaged over the perturber absolute velocity distribution (see for instance Refs. [120,121]). In cases where such inhomogenous processes have significant influence, the velocity averaged width does not provide the effective width of the profile and the question of what calculated quantity can be compared with measurements is then raised. Such a problem will be discussed, for the case of H_2O lines, in a future work.

4. Results for the fundamental bands

This section is devoted to tests of the model for individual lines of the fundamental bands. As explained above, only the transitions involving rotational levels with $Kc = J$ or $J - 1$ have been retained. Comparisons between measured and calculated values are presented below, provided that the number of measured lines was sufficient to cover a significant range of J values. Hence some of the retained series of lines may not be represented when there are too few data.

4.1. The ν_2 band

Collisional parameters of absorption lines in the ν_2 band for H_2O–N_2 and H_2O–air mixtures have received considerable experimental attention in the last 30 years due to the wide use of this spectral region for remote sensing. There are now more than three thousand measurements of room temperature broadening and fewer of pressure shifts gathered in about thirty references. The recent studies by Toth [92] and Zou et al. [12] bring the largest sets of data with more than 2000 and 300 determinations, respectively, but a number of references [51,72,80,90] also provide more than 50 measurements. In most cases, the lines retained for the present study have been measured by various authors so that the procedure (see Section 3.1) retained for the determination of the "experimental value" and of its uncertainty is reliable as illustrated by the examples in Table 1.

Results for the lines associated with levels with $Kc = J$ or $J - 1$ are displayed in Figs. 2–4. They are associated with $Kc = J$ P and R lines ($J \pm 1_{1,J\pm1} \leftarrow J_{0,J}$ and $J \pm 1_{0,J\pm1} \leftarrow J_{1,J}$ in Fig. 2), $Kc = J$ or $J - 1$ Q lines ($J_{1,J-1} \leftarrow J_{0,J}$ and $J_{0,J} \leftarrow J_{1,J-1}$, in Fig. 3) and $Kc = J - 1$ P and R lines ($J \pm 1_{2,J-1\pm1} \leftarrow J_{1,J-1}$ and $J \pm 1_{1,J-1\pm1} \leftarrow J_{2,J-1}$ in Fig. 4). These plots show that the overall

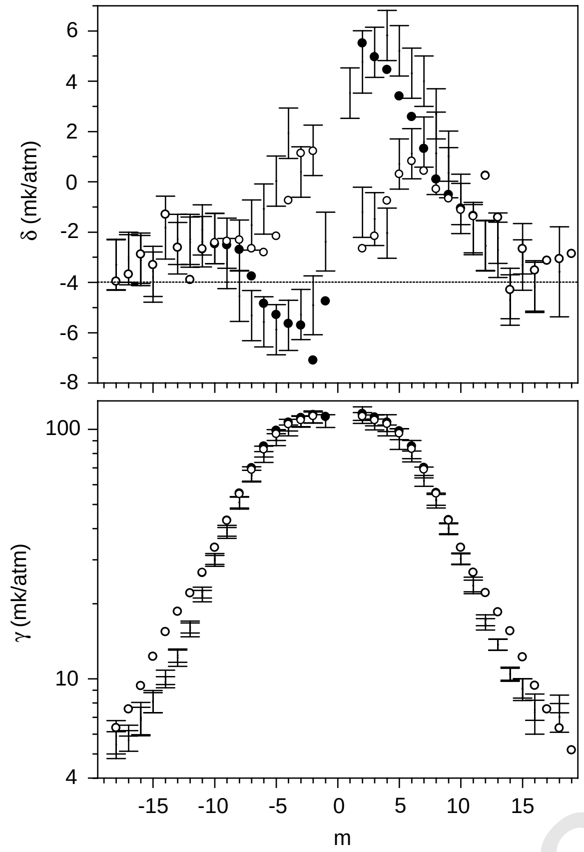

Fig. 2. Results obtained for the $Kc = J$ ($J \pm 1_{1,J\pm1} \leftarrow J_{0,J}$ and $J \pm 1_{0,J\pm1} \leftarrow J_{1,J}$) *P* and *R* doublets of the ν_2 band. *I* are experimental values. • and ○ are calculated values associated with *P* and *R* lines such that $(Ka' - Ka'') = (J' - J'')$ and $(Ka' - Ka'') = -(J' - J'')$, respectively. The horizontal dashed line indicates the pure dephasing contribution.

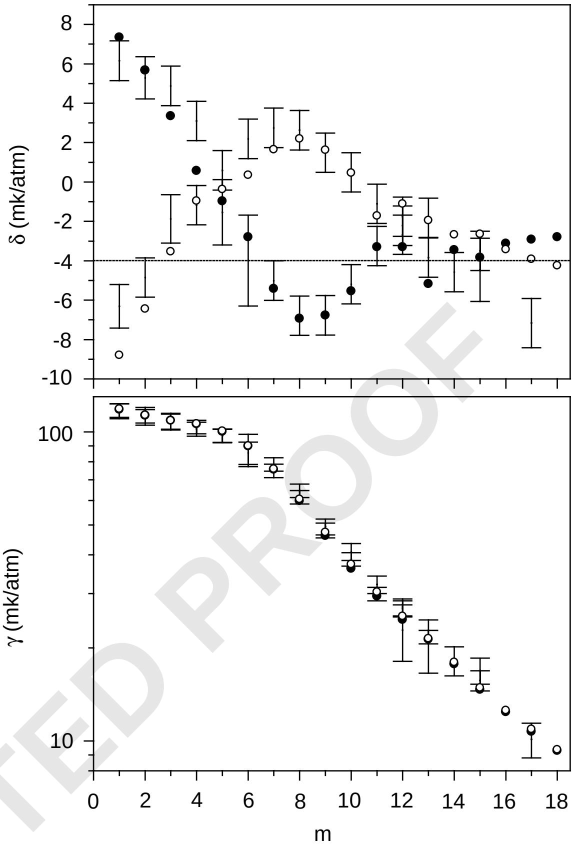

Fig. 3. Results obtained for the $Kc = J$ or $J - 1$ (the $J_{1,J-1} \leftarrow J_{0,J}$ and $J_{0,J} \leftarrow J_{1,J-1}$) Q line doublets of the ν_2 band. *I* are experimental values. • and ○ are calculated values of the $Ka' - Ka'' = 1$ and $Ka' - Ka'' = -1$ transitions, respectively. The horizontal dashed line indicates the pure dephasing contribution.

agreement between measured and calculated values is very satisfactory, for both the widths and the shifts.

The decrease of γ with increasing J, which reaches more than one order of magnitude, is correctly accounted for by our model. Predictions often agree with experimental determination of the broadening parameters within better than 5% and, in most cases, are within the uncertainties of the measurements, with the exception of the $Kc = J$ doublets with $J > 10$ (Fig. 2). This discrepancy is surprising in view of the quality of predictions obtained for the other doublets. Indeed, calculated values are precise for those with $Kc = J - 1$ (Fig. 4) but significantly overestimate the widths of the lines with $Kc = J$ although both types of transitions have similar broadenings. There are a number of possible explanations for this result. The first is, of course, a breakdown of the semiclassical model

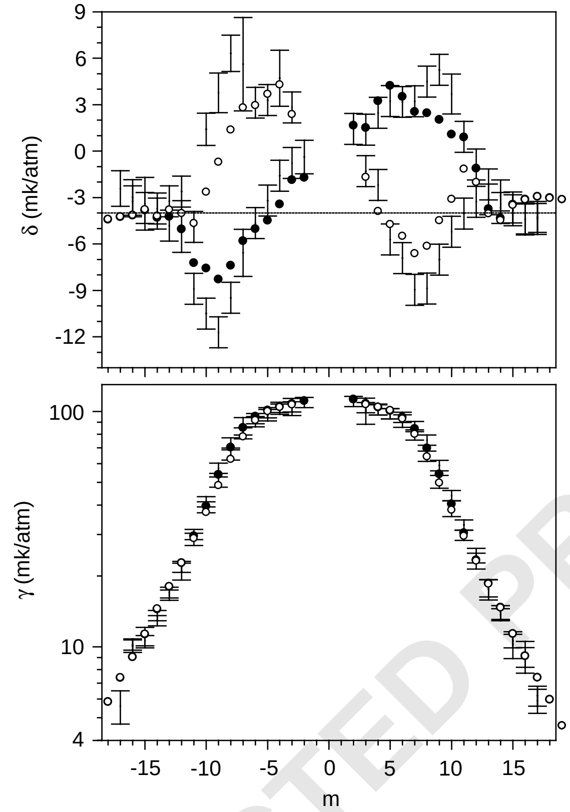

Fig. 4. Results obtained for the $Kc=J-1$ ($J\pm1_{2,J-1\pm1}\leftarrow J_{1,J-1}$ and $J\pm1_{1,J-1\pm1}\leftarrow J_{2,J-1}$) *P* and *R* doublets of the ν_2 band. *I* are experimental values. ● and ○ are calculated values associated with *P* and *R* line such that $(Ka'-Ka'')=(J'-J'')$ and $(Ka'-Ka'')=-(J'-J'')$, respectively. The horizontal dashed line indicates the pure dephasing contribution.

since the rotational changes induced by collisions involve, for these narrow lines, rotational energy jumps that are significant with respect to the kinetic energy. Nevertheless, such an explanation would also stand for the $Kc=J-1$ lines for which correct results are obtained. Besides this fundamental limitation of the model another explanation may be looked for in the imperfection of the potential parameters used. Indeed, a detailed look at Figs. 2 and 3 shows that changing the potential (atom–atom) parameters in order to predict values 10–15% lower for the high *J* lines would improve the results for those with $Kc=J$ and still lead to satisfactory results for the $Kc=J-1$ lines. Another possible source for the observed discrepancy is related with the narrowness of these lines and the fact that the two transitions composing the doublet ($Ka=J-Kc$ and $J-Kc+1$) are very closely spaced. This makes measurements difficult due to the small contribution of pressure broadening (with respect to the Doppler and instrument functions) and the strong overlap of the two lines. Furthermore, these transitions have profiles that are sensitive to collisional narrowing (e.g., Refs. [10,42,86,94] and those cited therein) and to the velocity averaging of the spectral shape [100]. In this case, the choice of a correct shape for the determination of line parameters from fits of measured spectra is not straightforward. Furthermore, as mentioned in the previous section, when velocity averaging has significant effects, the question of what quantity is retrieved from measurements and of what calculated value it should be compared with is not straightforward (this will be discussed in detail in a forthcoming paper). Finally note that widths of *P* and *R* transitions with identical quantum numbers ($f \leftarrow i$ and $i \leftarrow f$) are practically the same, and that, for high *J* values the widths of the two doublet transitions ($\Delta Ka = 1$ and -1) are practically equal as shown by both the measurements and calculations. This is expected since for large values of *J* and *Kc*, water vapor tends to be a symmetric top, *Kc* becomes a good quantum number and the levels associated with the two values of *Ka* (e.g., $15_{0,15}$ and $15_{1,15}$) have practically the same energy.

The quality of the predictions for the pressure shifts is worth noting. Indeed, the calculations account for most of the variations of δ with rotation quantum numbers and nicely follow the patterns drawn by the experimental results. As noted previously [92] and contrary to the widths, the pressure shifts for the $f \leftarrow i$ and $i \leftarrow f$ transitions show variations that are almost antisymmetric. On the other hand, as for γ, δ is the same for the two components of high *J* doublets.

As noted above, the shifts for *P* and *R* lines are almost opposite whereas the widths are similar. This result can be analyzed, following Ref. [2] by considering the quantities:

$$\frac{\gamma_{fi}+\gamma_{if}}{2}+i\frac{\delta_{fi}+\delta_{if}}{2}$$
$$=\left\langle 1-\frac{\exp[-{}^{R}S_2(fi)-i{}^{I}S_2(fi)-iS_1(fi)]+\exp[-{}^{R}S_2(if)-i{}^{I}S_2(if)-iS_1(if)}{2}\right\rangle,$$

$$\frac{\gamma_{fi}-\gamma_{if}}{2}+i\frac{\delta_{fi}-\delta_{if}}{2}$$
$$=\left\langle\frac{\exp[-{}^{R}S_2(if)-i{}^{I}S_2(if)-iS_1(if)]-\exp[-{}^{R}S_2(if)-i{}^{I}S_2(if)-iS_1(if)}{2}\right\rangle. \quad (11)$$

If one neglects spectroscopic differences between the lower and upper vibrational states, i.e. assuming that the rotational structures are similar in the $v_2 = 1$ and 0 states, one can easily show that

$${}^{R}S_2(if)={}^{R}S_2(fi),\quad {}^{I}S_2(if)=-{}^{I}S_2(fi),\quad \text{and}\quad S_1(if)=S_1(fi). \quad (12)$$

Using these relations, Eqs. (11) can then be written as

$$\frac{\gamma_{fi}+\gamma_{if}}{2}=\langle 1-\exp^{-{}^{R}S_2(fi)}\cos[{}^{I}S_2(fi)]\cos[S_1(fi)]\rangle,$$

$$\frac{\gamma_{fi}-\gamma_{if}}{2}=\langle \exp^{-{}^{R}S_2(fi)}\sin[{}^{I}S_2(fi)]\sin[S_1(fi)]\rangle,$$

$$\frac{\delta_{fi}+\delta_{if}}{2}=\langle \exp^{-{}^{R}S_2(fi)}\cos[{}^{I}S_2(fi)]\sin[S_1(fi)]\rangle,$$

$$\frac{\delta_{fi}-\delta_{if}}{2}=\langle \exp^{-{}^{R}S_2(fi)}\sin[{}^{I}S_2(fi)]\cos[S_1(fi)]\rangle. \quad (13)$$

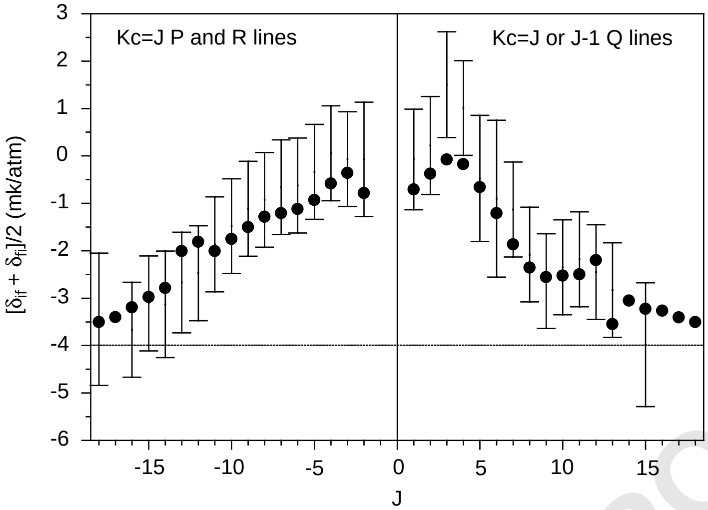

Fig. 5. Half sum of the experimental (I) and calculated (●) shifts for lines with identical rotational quantum numbers in the ν_2 band. Results obtained for Q lines ($[\delta(J_{1,J-1} \leftarrow J_{0,J}) + \delta(J_{0,J} \leftarrow J_{1,J-1})]/2$) are given for positive values of J, whereas those obtained from P and R lines with $Kc = J$ ($[\delta(J+1_{1,J+1} \leftarrow J_{0,J}) + \delta(J_{0,J} \leftarrow J+1_{1,J+1})]/2$) are displayed for negative J values. The horizontal dashed line indicates the pure dephasing contribution.

Since ${}^{I}S_2$ is small, as is S_1 for lines of the ν_2 band due to the small effect of the bending vibration on the induction and dispersion interaction potential, these equations can be approximated, to first order, by

$$\begin{aligned}
&\frac{\gamma_{fi}+\gamma_{if}}{2} \approx \langle \exp[-{}^{R}S_2(fi)]\rangle = {}^{\mathrm{Rot}}\gamma_{fi} = {}^{\mathrm{Rot}}\gamma_{if},\\
&\frac{\gamma_{fi}-\gamma_{if}}{2} \approx 0,\\
&\frac{\delta_{fi}+\delta_{if}}{2} \approx \langle \exp[-{}^{R}S_2(fi)] \times S_1(fi)\rangle,\\
&\frac{\delta_{fi}-\delta_{if}}{2} \approx \langle \exp[-{}^{R}S_2(fi)] \times {}^{I}S_2(fi)\rangle = {}^{\mathrm{Rot}}\delta_{fi} = -{}^{\mathrm{Rot}}\delta_{if},
\end{aligned} \tag{14}$$

where values with the superscript “Rot” designate those for purely rotational lines. These expressions explain the symmetry of the widths in the P and R branches and indicate that, in the absence of vibrational dephasing ($S_1 = 0$), P and R lines have opposite shifts. Note that, although small, the effects of vibration through the S_1 contribution are discernible in the ν_2 band as shown by the non zero values of ($\delta_{fi} + \delta_{if}/2$) in Fig. 5. For very narrow lines, ${}^{R}S_2$ and ${}^{I}S_2$ are almost zero and the shifts then become independent on rotational quantum numbers and equal to $\langle S_{1fi}\rangle$. This situation, which has been observed in the case of HF [1,2], is not reached here (see Fig. 5), even for the high J lines, since the rotational contribution to the broadening remains significant.

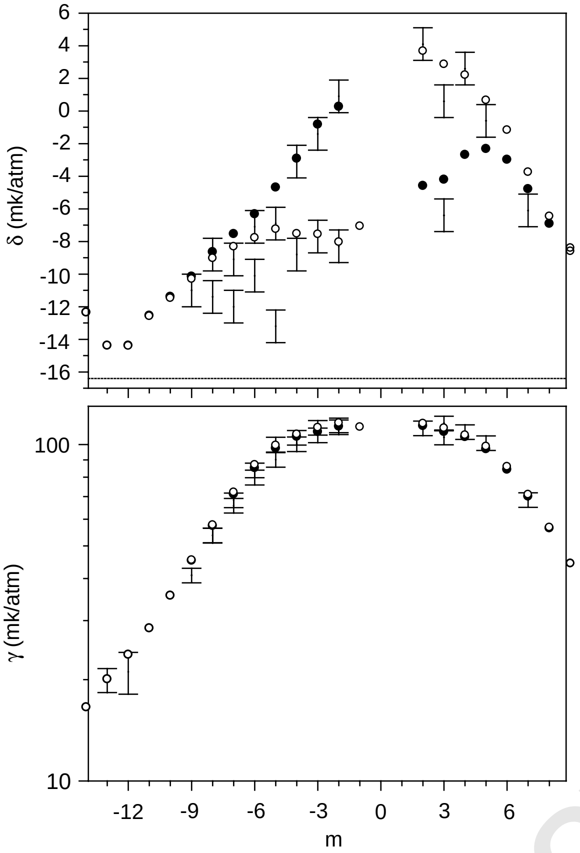

Fig. 6. Results obtained for the $Kc=J$ P and R doublets of the ν_1 band. Same legend and symbols as in Fig. 2.

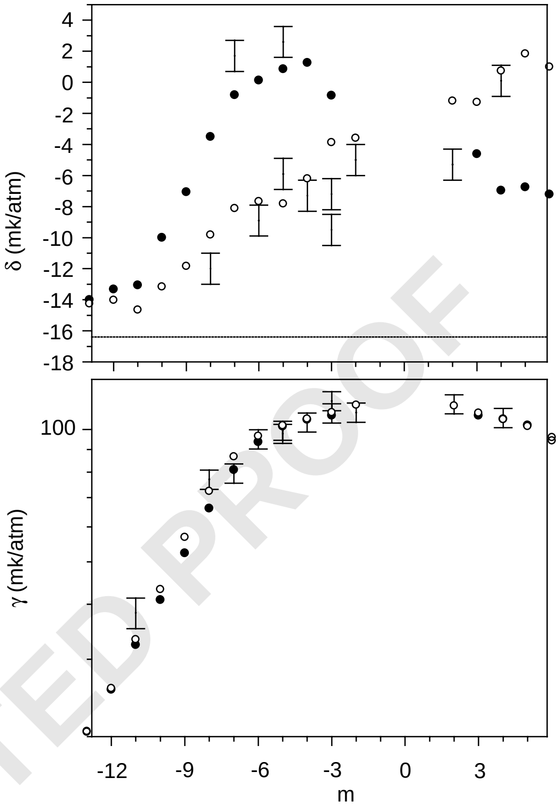

Fig. 7. Results obtained for the $Kc=J-1$ P and R doublets of the ν_1 band. Same legend and symbols as in Fig. 4.

4.2. The ν_1 band

The situation in the ν_1 band is much less favorable in terms of measured data than in the ν_2 band since, for the doublet transitions studied here, most lines have only been measured once [12]. The results obtained for the available P and R transitions with $Kc = J$ and $J - 1$ are plotted in Figs. 6 and 7. They are qualitatively similar to those obtained in the case of ν_2 lines except for the line shifts which are significantly more negative. This is expected [see Eq. (8)] since stretching vibrations have larger effects than the bending mode on the water polarizability [see Eq. (4)] and thus lead to larger S_1 contributions [Eq. (10)]. Some significant differences between measured and calculated shifts appear, as for $m = -5$ in Fig. 6, whose analysis is difficult in the absence of any measurement confirming that of Ref. [12].

4.3. The ν_3 band

The situation in the ν_3 band is, again, less favorable than in the ν_2 band, but slightly better than in ν_1 due to the experiments of Refs. [12,75]. Measured and calculated values for P and R doublets

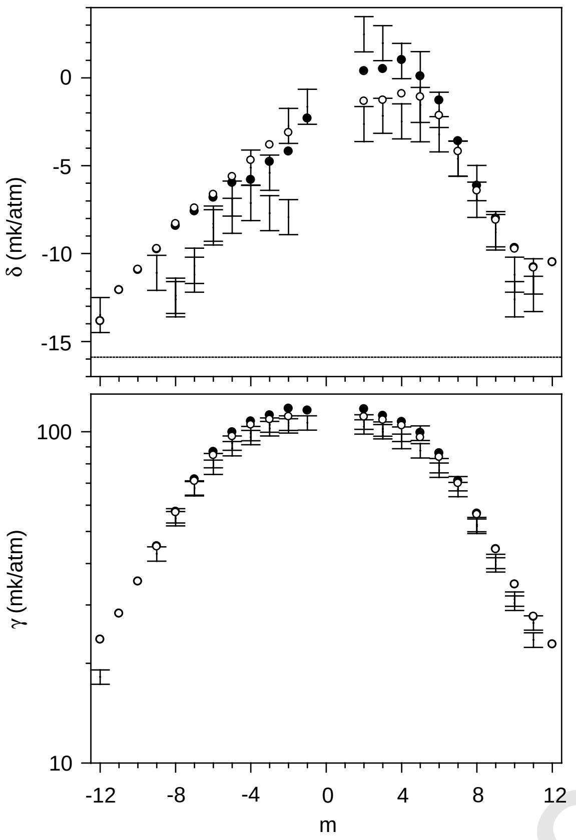

Fig. 8. Results obtained for the $Kc=J$ ($J\pm1_{0,J\pm1}\leftarrow J_{0,J}$ and $J\pm1_{1,J\pm1}\leftarrow J_{1,J}$) P and R doublets of the ν_3 band. I are experimental values. ● and ○ are calculated values associated with P and R line with $Ka=0$ and 1, respectively. The horizontal dashed line indicates the pure dephasing contribution.

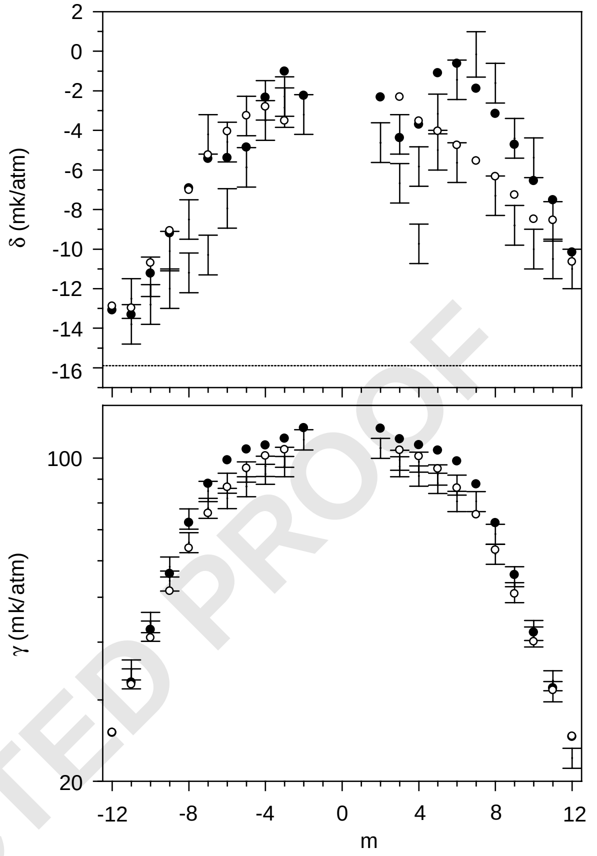

Fig. 9. Results obtained for the $Kc=J-1$ ($J\pm1_{1,J-1\pm1}\leftarrow J_{1,J-1}$ and $J\pm1_{2,J-1\pm1}\leftarrow J_{2,J-1}$) P and R doublets of the ν_3 band. I are experimental values. ● and ○ are calculated values associated with P and R line with $Ka=1$ and 2, respectively. The horizontal dashed line indicates the pure dephasing contribution.

can be compared in Figs. 8 and 9. Again, the widths are very similar to those in the ν_2 and ν_1 bands whereas the shifts are more pronounced than in ν_2 and quite similar to those of ν_1 lines as expected from the values in Eqs. (4) and (10). As for ν_2 lines (Fig. 5), we have calculated the half sum of shifts of P and R lines with identical rotational quantum numbers. The results, shown in Fig. 10, together with the shifts plotted in Figs. 8 and 9 validate the ab-initio values of the derivative of polarizability with respect to the ν_3 mode.

4.4. Vibrational effects

The effects of the vibration on the shifts are large as has been well known for many years and confirmed by the preceding results. On the other hand, the question of differences between

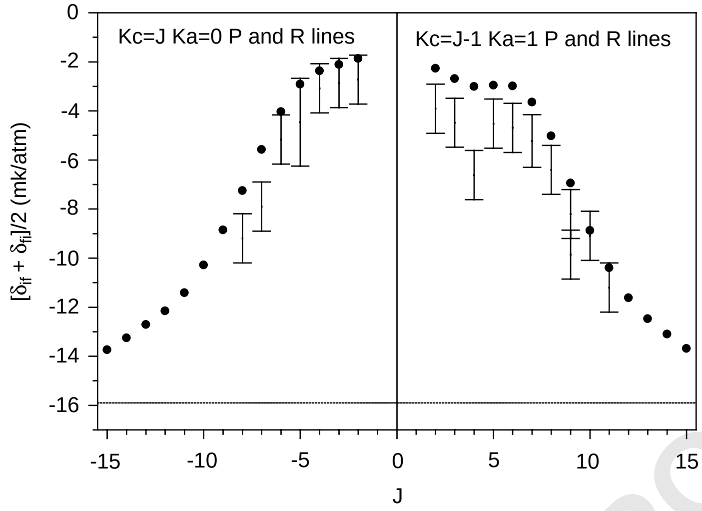

Fig. 10. Half sum of the experimental (I) and calculated (●) shifts for P and R lines with identical rotational quantum numbers in the ν_3 band. Results obtained the $Kc=J$ transitions ($[\delta(J+1_{0,J+1}\leftarrow J_{0,J})+\delta(J_{0,J}\leftarrow J+1_{0,J+1})]/2$) are given for negative values of J, whereas those obtained $Kc=J-1$ transitions ($[\delta(J+1_{1,J}\leftarrow J_{1,J-1})+\delta(J_{1,J-1}\leftarrow J+1_{1,J})]/2$) are displayed for positive J values. The horizontal dashed line indicates the pure dephasing contribution.

line-broadening parameters of the fundamental bands, raised by many authors, has not yet been answered conclusively. As discussed in the introduction, the studies of Refs. [11,12] seem to indicate that widths are larger in the pure rotational and ν_1 band than in the ν_2 band (although differences are generally smaller than 10% and might be within experimental errors). In order to analyze the reasons for these differences, we have compared calculated widths in the all three bands using the ground state wavefunctions and energies for all levels. The differences in the broadening coefficients for the doublet lines studied here, which arise from the contribution of S_1, were found to be negligible. This shows that the vibrational dependence of the potential is too weak to induce significant effects when only a single vibrational quantum is involved. We then made calculations with the proper wavefunctions and rotational energies but using the same potential for all three bands (setting the S_1 term to zero). The calculated values, which then show the effects of the spectroscopic structure, are displayed in Fig. 11 for the doublet lines under study here. They confirm that lines of the ν_2 band are narrower than both those of the purely rotational and ν_1 transitions. This result and the range of values obtained are consistent with the conclusions of Ref. [11] as is the fact that the ratio $\gamma(\mathrm{rot})/\gamma(\nu_2)$ is, on the average smaller than $\gamma(\nu_1)/\gamma(\nu_2)$. Note that calculations of self broadening coefficients made about 20 years ago by Mandin et al. [122] had also shown that using proper wavefunctions and energies for the $v_2=1$ levels leads to a reduction of the widths when compared with those predicted using only ground state data. Analysis of this result shows that it is mostly due to differences in the rotational energies of the levels. Indeed, the $v_2=1$ state has a rotational constant A (≈ 31 cm^{-1}) that is significantly larger than that of the ground and $v_1=1$ states (≈ 27 cm^{-1}). This leads to larger energy gaps between the collisionally connected states. Hence collisions, particularly for high J lines with small widths, are less resonant in the bending state leading to smaller widths.

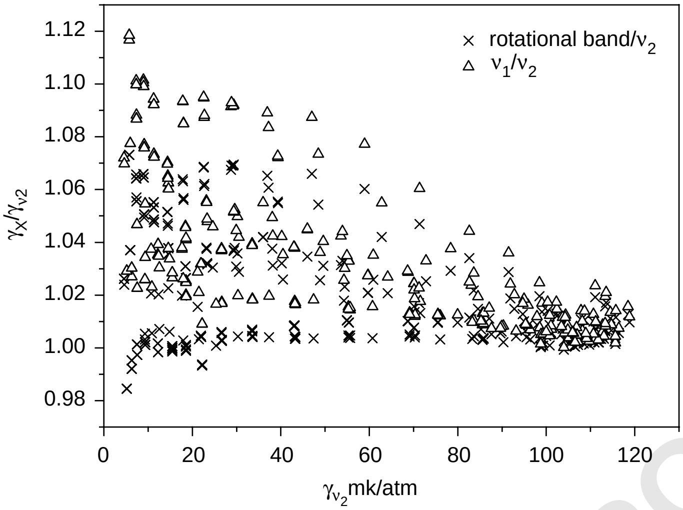

Fig. 11. Ratios of calculated H_2O–N_2 widths of the rotational and ν_2 lines (×) and of the ν_1 and ν_2 lines (△) for the $Kc = J$ and $J - 1$ transitions.

5. Highly excited overtones

The preceding results show that spectroscopic effects on the widths are relatively small (typically less than 10%) and thus quite difficult to detect without ambiguity due the experimental uncertainties. They also indicate that the vibrational dependence of the potential leads to significant changes for the shifts of line of the fundamental bands but has negligible influence on the widths. Nevertheless, one should recall [see Eq. (10)] that the S_1 term depends linearly on the numbers of excited vibrational quanta and that its contributions to the shifting and broadening are linear and quadratic, respectively. The effects of vibration on the widths, through the potential, will then be four times larger in $2\nu_1$ than in ν_1 and 25 times larger for $5\nu_1$ (two and five times larger when the shifts are considered). Furthermore, due to the variations of polarizability with respect to the vibrational modes, a change of n quanta leads to values of $(S_1)^2$ that are similar in both stretching modes and about 20 times larger that those obtain for n quanta of the bending vibration. Hence high J lines of highly excited stretching overtone transitions are likely suitable for the detection of significant differences in the widths with respect to those of weakly excited lines. This is clear from the calculated values of Fig. 12 which also confirm the remark of Section 3.2 stating that effects are masked for broad (low J) lines.

Comparisons between measured and calculated H_2O–N_2 line widths in the $3\nu_1+\nu_3$ and $2\nu_1+2\nu_2+\nu_3$ bands have been made previously [17]. They have shown the quality of the approach and the precision of the predicted values of the shifts are a further confirmation of the quality of the dependence of polarizability on v_1 and v_3 in Eq. (4). Since there is relatively little data for the $Kc = J$ and $J - 1$ lines high overtones, we have grouped them in order to carry the procedure described in Section 3.2. While doing this, we have selected only transitions starting from the ground vibrational state in which the upper state has no quanta in v_2 and a given total number of quanta of stretching vibrations (i.e., given values of $v_1' + v_3' = \Delta v_1 + \Delta v_3$). This procedure, which enlarges the data sets, is valid

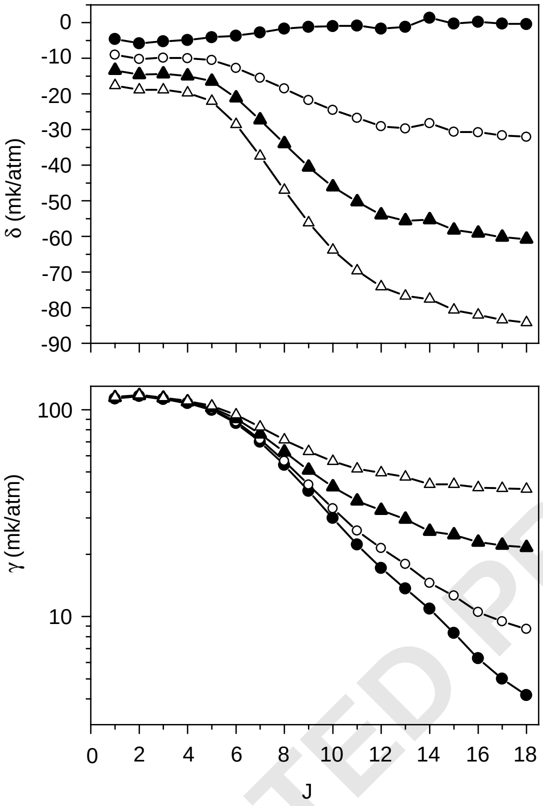

Fig. 12. Calculated H_2O–N_2 widths and shifts for the $J-1_{0,J-1} \leftarrow J_{1,J}$ transitions of the rotational (●), $2\nu_1$ (○), $4\nu_1$ (▲) and $6\nu_1$(△) bands.

since both stretching vibrations have similar effects on the vibrational dependence of the potential and since spectroscopic effects on the widths are small.

5.1. Three and four quanta of stretching vibration

Comparisons between measured and calculated widths for doublet lines with $Kc = J$ and $J-1$ in overtones involving three quanta of stretching vibration are plotted in Figs. 13 and 14. Although there is some significant scatter, the agreement between experiments and predictions is satisfactory and these results clearly demonstrate the effects of vibration. Indeed, the calculation made for the fundamental bands (validated in Section 4) significantly underestimated the widths of high J lines whereas calculated results for three quanta lead to much better agreement. Note that, for $Kc = J = 15$, the vibrational dependence of the potential increases the width by a factor of practically two. This demonstration of the effects of vibration is further confirmed when transitions with four quanta are considered as shown by the results of Figs. 15 and 16. Unfortunately, for such high overtones high J lines have not been studied.

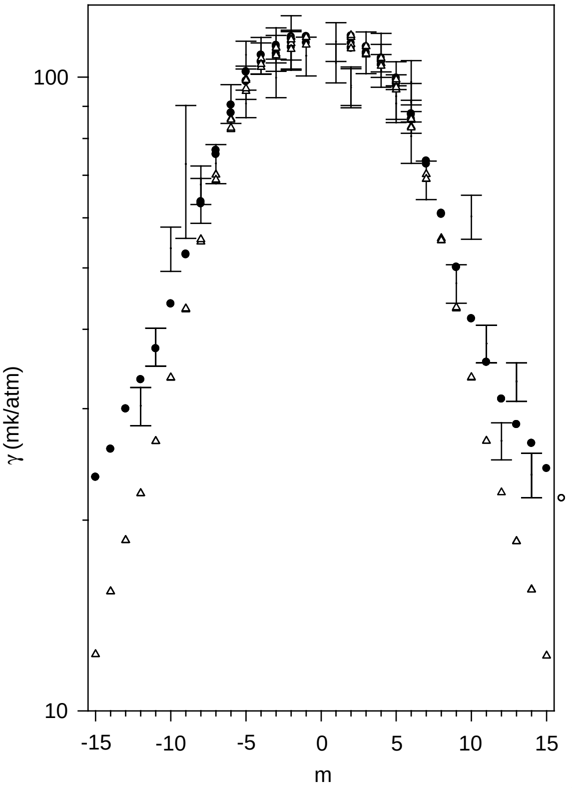

Fig. 13. H_2O–N_2 widths for transitions with $Kc = J$ in bands involving three quanta of stretching vibration. I are experimental values whereas ● and △ are values calculated in the considered band and in the v_2 band, respectively.

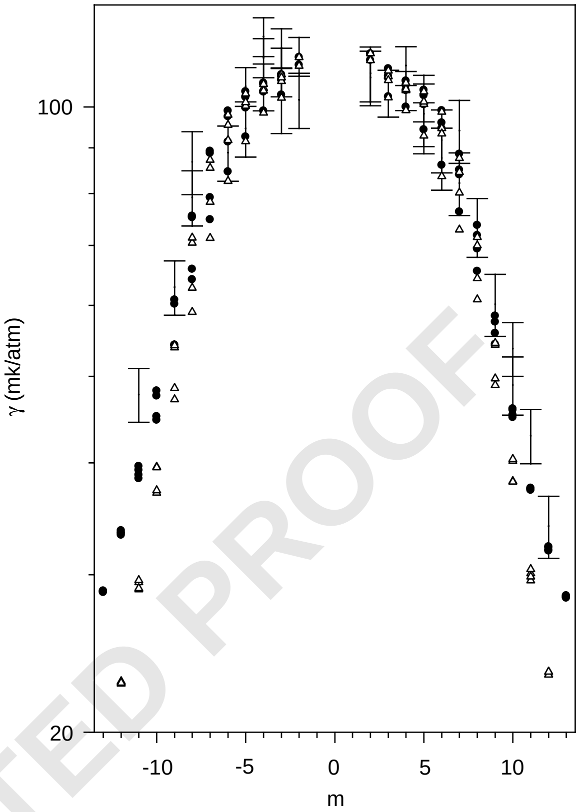

Fig. 14. Same as Fig. 13 but for $Kc = J - 1$ transitions.

5.2. Dependence for specific transitions

Starting from Eq. (8), for a transitions involving various vibrational states but specific sets i and f of rotational quantum numbers one should have, in the absence of spectroscopic effects, the following dependence on vibration quantum numbers:

$$\gamma[(v_1', v_2', v_3')f \leftarrow (v_1'', v_2'', v_3'')i] = \gamma^0_{f\leftarrow i} + A_{f\leftarrow i} \times (0.3\Delta v_1 + 0.07\Delta v_2 + 0.3\Delta v_3)^2,$$

$$\delta[(v_1', v_2', v_3')f \leftarrow (v_1'', v_2'', v_3'')i] = \delta^0_{f\leftarrow i} + B_{f\leftarrow i} \times (0.3\Delta v_1 + 0.07\Delta v_2 + 0.3\Delta v_3). \qquad (15)$$

For a check of this relation with have retained transitions with $Kc = J$. In order to have sufficient sets of data, we have retained both P and R lines with the same value of $|m|$ and all lines with $\Delta Ka = 0, \pm 1$. Measured and calculated widths and shifts for specific lines are plotted in Figs. 17 and 18. These confirm the quality of the present calculations, the validity of the relations in Eqs.

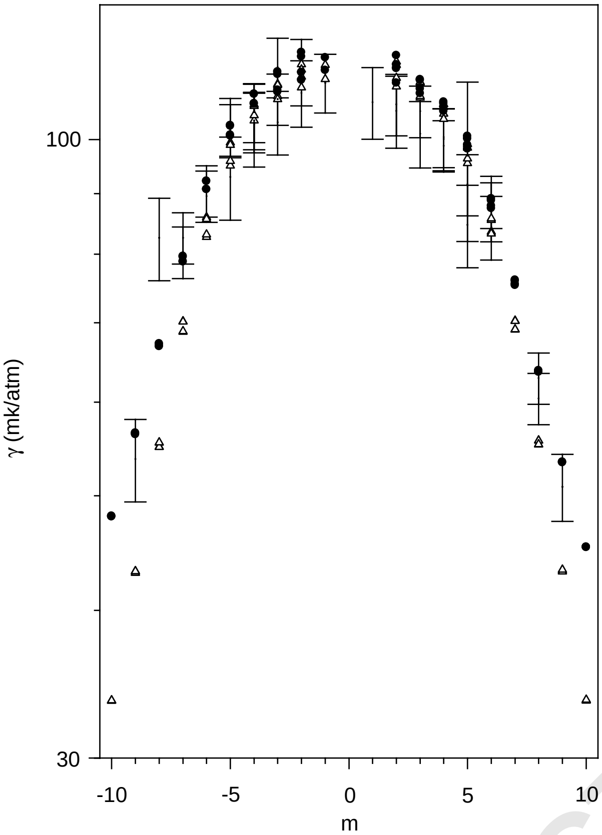

Fig. 15. H_2O–N_2 widths for transitions with $Kc = J$ in bands involving four quanta of stretching vibration. I are experimental values whereas ● and △ are values calculated in the considered band and in the ν_2 band, respectively.

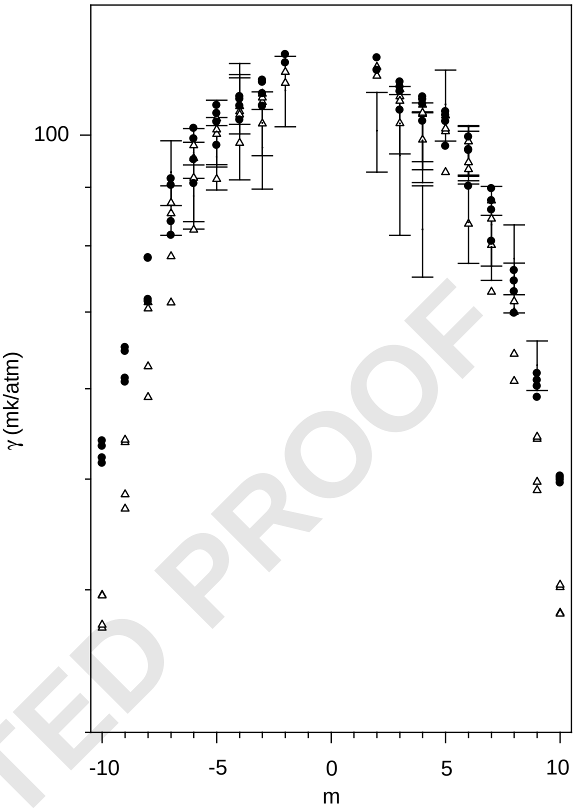

Fig. 16. Same as Fig. 15 but for $Kc = J - 1$ transitions.

(15), and clearly demonstrate that there is, indeed, a significant vibrational dependence of the line widths that is correctly predicted by our theoretical approach.

6. Conclusion

The present study, devoted to the room temperature broadening and shifting of H_2O lines by N_2 has demonstrated the quality of the semi-classical model used. Indeed, the latter was proved to correctly predict the large variations of the widths from low to high J lines as well as most of the specific structures showed by the variations of the shifts with rotational quantum numbers. Furthermore, use of both measured and calculated collisional line parameters for properly selected lines has enabled, for the first time, a clear demonstration of the vibrational dependences of both the shifts and widths. It was shown that differences in the broadening and shifting of lines of iden-

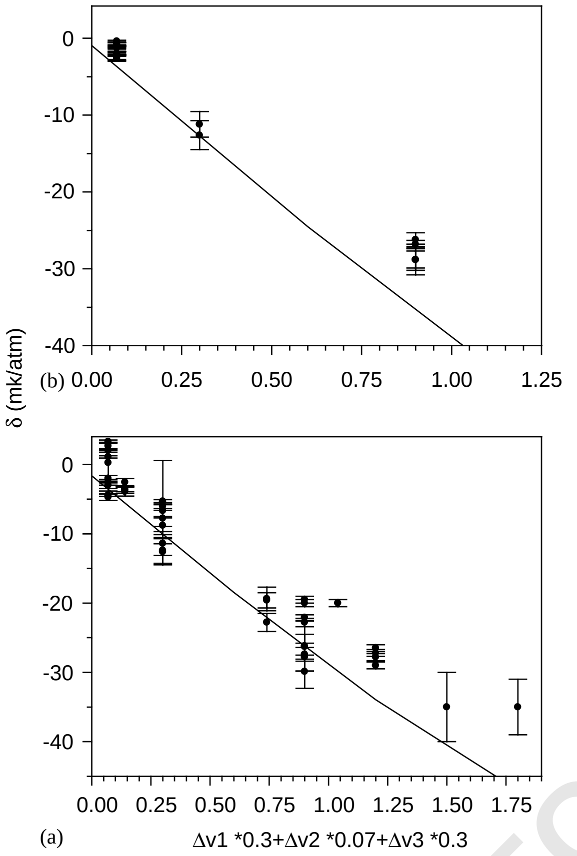

Fig. 17. Measured (●) and calculated (—) shifts for *P* and *R* transitions with $Kc=J$ in various bands. (a) $|m|=8$ lines (b) $|m|=10$ lines. Each plot includes available results for the $|m|-1_{Ka',|m|-1} \leftrightarrow |m|_{Ka,|m|}$ with $Ka=0,1$ and $Ka'=0,1$.

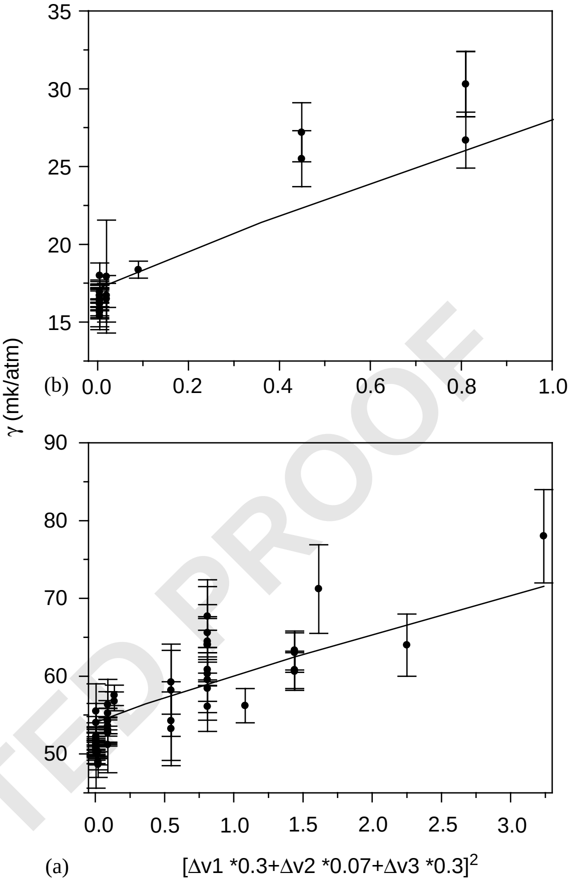

Fig. 18. Measured (●) and calculated (—) widths for *P* and *R* transitions with $Kc=J$ in various bands. (a) $|m|=8$ lines (b) $|m|=12$ lines. Each plot includes available results for the $|m|-1_{Ka',|m|-1} \leftrightarrow |m|_{Ka,|m|}$ with $Ka=0,1$ and $Ka'=0,1$.

tical rotational states in different bands arise from both spectroscopic differences and the vibrational dependence of the potential. The first effect, although small should be discernable using modern spectroscopy experimental tools by studying high *J* lines of the pure rotation (or v_1) and v_2 bands. The second effect is easier to detect and was clearly proved here since it increases quickly with the number of quanta of stretching vibration. Note that calculated values indicate that the width of the $14_{1,14} \leftarrow 13_{0,13}$ transition, for instance, should change by a factor of more than two when going from v_1 to $4v_1$ and a factor of four in the case of $6v_1$. Precise measurements for high $Kc=J$ doublets of very excited overtone transitions are still missing and would be of considerable interest in order to further confirm the conclusions of the present study.

All calculations presented in this paper were made disregarding any averaging on the velocity v and only using the mean thermal velocity. The high *J* doublets lines considered here are very narrow since the associated rotational jumps induced by collisions are well off-resonance. Indeed, a large resonance parameter, $k_{\mathrm{res}} = |\Delta E_{i,i'} + \Delta E_{J_2,J_2'}| \times b/v$, leads to small values of the resonance functions $F_n(k_{\mathrm{res}})$. Since the latter decrease quickly with increasing k_{res} [28], their values for lines involving high rotational states should be very dependent on the velocity v. Hence the widths and shifts of high J doublets should have very strong dependences on both v and, consecutively "abnormal" dependences on temperature as pointed out in Ref. [63]. Furthermore, inhomogeneous effects related with the velocity averaging [120,121] should be strong as indicated by the results of Ref. [100]. Finally, such effects should be quite different in fundamental and overtone bands due to differences in the contribution of the S_1 term which is purely resonant. A study of the influence of the velocity averaging (and of temperature) on the widths and shifts of H_2O lines in various bands will be the subject of a forthcoming work.

Acknowledgements

One of the authors (RRG) is pleased to acknowledge support of this research by the National Science Foundation through Grant No. ATM-9415454. Any opinions, findings, and conclusions or recommendations expressed in this material are those of the author(s) and do not necessarily reflect the views of the National Science Foundation.

References

[1] Grigoriev IM, Le Doucen R, Boissoles J, Calil B, Boulet C, Hartmann JM, Bruet X, Dubernet ML. Spectral lineshape parameters revisited for HF in a bath of argon. I. Widths and shifts in the (0-0), (0-1), and (0-2) band. J Mol Spectrosc 1999;198:249–56.

[2] Hartmann JM, Boulet C. Line shape parameters for HF in a bath of argon as a test of classical path models. J Chem Phys 2000;113:9000–10.

[3] Roche CF, Hutson JM, Dickinson AS. Calculations of line width and shift cross sections for HCl in Ar. JQSRT 1995;53:153–64.

[4] Gamache RR, Hartmann JM, Rosenmann L. Collisional broadening of water–vapor lines: I. A survey of experimental results. JQSRT 1994;52:481–99.

[5] Smith MAH, editor., NASA Conference Publication 2396, NASA, Scientific and Technical Information Branch, 1985.

[6] Atmospheric Spectroscopy Applications Workshop, ASA REIMS 96, Université de Reims, Champagne Ardenne, Sept. 4–6, 1996.

[7] Smith MAH, editor. Third Langley spectroscopic parameters workshop, NASA Langley Research Center, Hampton, VA, 1992.

[8] Mandin JY, Chevillard JP, Flaud JM, Camy-Peyret C. N_2-broadening coefficients of $H_2^{16}O$ lines between 8500 and 9300 cm^{-1}. J Mol Spectrosc 1988;132:352–60.

[9] Mandin JY, Chevillard JP, Flaud JM, Camy-Peyret C. N_2-broadening coefficients of $H_2^{16}O$ lines between 9500 and 11 500 cm^{-1}. J Mol Spectrosc 1989;138:272–81.

[10] Grossmann BE, Browell EV. Water–vapor line broadening and shifting by air, nitrogen, oxygen, and argon in the 720-nm Wavelength Region. J Mol Spectrosc 1989;138:562–95.

[11] Brown LR, Plymate C. H_2-broadened $H_2^{16}O$ in four infrared bands between 55 and 4045 cm^{-1}. JQSRT 1996;56: 263–82.

[12] Zou Q, Varanasi P, Laboratory measurement of the spectroscopic line parameters of water vapor in the 950–2100 and 3000–4050 cm^{-1} regions at lower-tropospheric temperatures. JQSRT 2002, in press.

[13] Rothman LS, Rinsland CP, Goldman A, Massie ST, Edwards DP, Flaud JM, Perrin A, Dana A, Mandin JY, Schroeder J, McCann A, Gamache RR, Wattson RB, Yoshino K, Chance KV, Jucks KW, Brown LR, Nemtchinov V, Varanasi P. The HITRAN molecular spectroscopic database and HAWKS (HITRAN atmospheric workstation)(1996 Edition). JQSRT 1998;60:665–10.

[14] Lynch R, Gamache RR, Neshyba SP. Fully complex implementation of the Robert–Bonamy formalism: halfwidths and line shifts of H_2O broadened by N_2. J Chem Phys 1996;105:5711–21.

[15] Gamache RR, Lynch R, Neshyba SP. New developments in the theory of pressure-broadening and pressure-shifting of spectral lines of H_2O: The complex Robert–Bonamy formalism. JQSRT 1998;59:319–35.

[16] Lynch R, Gamache RR, Neshyba SP. N_2 and O_2 induced halfwidths and line shifts of water vapor transitions in the (301) ← (000) and (221) ← (000) bands. JQSRT 1998;59:595–613.

[17] Lynch R. PhD dissertation. Physics Department, University of Massachusetts Lowell, June 1995.

[18] Baranger M. General impact theory of pressure broadening. Phys Rev 1958;112:855–65.

[19] Kolb AC, Griem HR. Theory of line broadening in multiplet spectra. Phys Rev 1958;111:514–21.

[20] Griem H. Plasma spectroscopy. NY: McGraw Hill, 1964.

[21] Kubo R. Generalized cumulant expansion method. J Phys Soc Japan 1962;17:1100–20.

[22] Robert D, Bonamy J. Short range force effects in semiclassical molecular line broadening calculations. J de Phys 1979;40:923–43.

[23] Korff D, Leavitt RP. Calculation of impact broadened half width parameters for HCl using a natural cutoff theory. Phys Lett A 1975;53:351–2.

[24] Leavitt RP, Korff D. Cutoff-free theory of impact broadening and shifting in microwave and infrared spectra. J Chem Phys 1981;74:2180–8.

[25] Looney JP, Herman RM. Air broadening of the hydrogen halides. I. Theoretical determination with the temperature dependence of nitrogen broadening and shifting in the fundamental band of HCl. JQSRT 1987;37:547–57.

[26] Anderson PW. Dissertation, Harvard University, 1949.

[27] Anderson PW. Pressure broadening in the microwave and infra-red regions. Phys Rev 1949;76:647–61. Pressure broadening of the ammonia inversion line by foreign gases: quadrupole-induced dipole transitions. Phys Rev 1950;80:511–3.

[28] Tsao CJ, Curnutte Jr B. Line-widths of pressure-broadened spectral lines. JQSRT 1962;2:41–91.

[29] Lennard-Jones JE. On the determination of molecular fields.-II From the equation of state of a gas. Proc Roy Soc 1924;A106:463–77.

[30] Neshyba SP, Lynch R, Gamache RR, Gabard T, Champion JP. Pressure induced widths and shifts for the v_3 band of methane. J Chem Phys 1994;101:9412–21.

[31] Oka T. In: Bates DR, editor. Advances in atomic and molecular physics. New York: Academic Press, 1973.

[32] Ben-Reuven A. Spectral line shapes in gases in the binary-collision approximation. In: Prigogine I, Rice SA, editors. Advances in Chemical Physics, vol. 20. New York: Academic Press, 1975. p. 235.

[33] Shostak SL, Muenter JS. The dipole moment of water. II. Analysis of the vibrational dependence of the dipole moment in terms of a dipole moment function. J Chem Phys 1991;94:5883–90.

[34] Luo Y, Agren H, Vahtras O, Jorgensen P, Spirko V, Hettema H. Frequency-dependent polarizabilities and first hyperpolarizabilities of H_2O. J Chem Phys 1993;98:7159–64.

[35] Gray CG, Gubbins KE. Theory of molecular fluids. Oxford: Clarendon Press, 1984. p. 575.

[36] Neshyba SP, Gamache RR. Improved line broadening coefficients for asymmetric rotor molecules: application to ozone perturbed by nitrogen. JQSRT 1993;50:443–53.

[37] Hirschfelder JO, Curtiss CF, Bird RB. Molecular theory of gases and liquids. New York: Wiley, 1964.

[38] Good RJ, Hope CJ. Test of combining rules for intermolecular distances, potential function constants from second virial coefficients. J Chem Phys 1971;55:111–6.

[39] Sack RA. Two-center expansion for the powers of the distance between two points. J Math Phys 1964;5:260–8.

[40] Labani B, Bonamy J, Robert D, Hartmann JM, Taine J. Collisional broadening of rotation-vibration lines for asymmetric top molecules. I. Theoretical model for both distant and close collisions. J Chem Phys 1986;84: 4256–67.

[41] Hartmann JM, Gamache RR. A survey of measured half-widths and line shifts of water vapor. Work in progress, 2002.

[42] Eng RS, Calawa AR, Harman TC, Kelley PL, Javan A. Collisional narrowing of infrared water–vapor transitions. Appl Phys Lett 1972;21:303–5.

[43] Blum FA, Nill KW, Kelley PL, Calawa AR, Harman TC. Tunable infrared laser spectroscopy of atmospheric water vapour. Science 1972;177:694–5.

[44] Ryadov VY, Furashov NI. Measurement of the parameters of the absorption line $\lambda_{ij} = 398$ μm in the rotational spectrum of water vapor. Opt Spectrosc 1973;35:255–7.

[45] Toth RA. Strengths and air-broadened widths of H_2O lines in the 2950–3400 cm^{-1} region. JQSRT 1973;13:1127–42.

[46] Eng RS, Kelley PL, Mooradian A, Calawa AR, Harman TC. Tunable laser measurements of water vapor transitions in the vicinity of 5 μm. Chem Phys Lett 1973;19:524–8.

[47] Eng RS, Kelley PL, Calawa AR, Harman TC, Nill KW. Tunable diode laser measurements of water vapour absorption line parameters. Molec Phys 1974;28:653–64.

[48] Ryadov VY, Furashov NI. On widths and intensities of submillimetre absorption lines of water vapour rotating spectrum. Radiophys Quantum Electron 1975;18:256–66.

[49] Guerra MA, Ketabi M, Sanchez A, Feld MS, Javan A. Water vapor spectroscopy at 5 μm using a tunable SFR laser. J Chem Phys 1975;63:1317–9.

[50] Cardinet P, Severin F, Valentin A, Claude ML, Henri A. Wavenumber, intensity and width of water vapour lines in the region of 5.3 μm. CR Acad Sc Paris 1977;284:37–9.

[51] Chang YS, Shaw JH. Intensities and widths of H_2O lines between 1800 and 2100 cm^{-1}. JQSRT 1977;18:491–9.

[52] Kasuga T, Kuze H, Shimizu T. Determinations of relaxation rate constants on the 22 GHz rotational transition of H_2O by coherent transient spectroscopy. J Chem Phys 1978;69:5195–8.

[53] Godlevskii AP, Kapitanov VA. Changes in the line shapes of water vapor due to broadening by foreign gases. J Appl Spectrosc 1978;28:142–6.

[54] Eng RS, Mantz AW. Tunable diode laser measurement of water vapor line parameters in the 10- to 15-μm spectral region. J Mol Spectrosc 1979;74:388–99.

[55] Wilkerson TD, Schwemmer G, Gentry B, Giver LP. Intensities and N_2 collision-broadening coefficients measured for selected H_2O absorption lines between 715 and 732 nm. JQSRT 1979;22:315–31.

[56] Giver LP, Gentry B, Schwemmer G, Wilkerson TD. Water absorption lines, 931–961 nm: selected intensities, N_2-collision-broadening coefficients, self-broadening coefficients, and pressure shifts in air. JQSRT 1982;27:423–36.

[57] Mucha JA. Tunable diode laser measurements of water vapor line parameters in the 6-μm spectral region. Appl Spectrosc 1982;36:141–7.

[58] Malathy Devi V, Fridovich B, Jones GD, Snyder DGS. Intensities and half-widths for several H_2O ν_2 lines in the region 1500–1523 cm^{-1}. J Mol Spectrosc 1985;111:114–8.

[59] Bauer A, Godon M, Duterage B. Self- and air-broadened linewidth of the 183 GHz absorption in water vapour. JQSRT 1985;33:167–75.

[60] Cahen C, Grossmann BE, Lesne JL, Benard J, Leboudec G. Intensities and atmospheric broadening coefficients measured for O_2 and H_2O absorption lines selected for DIAL monitoring of both temperature and humidity. II. H_2O. Appl Opt 1986;25:4268–71.

[61] Malathy Devi V, Benner DC, Rinsland CP, Smith MAH, Sidney BD. Diode laser measurements of air and nitrogen broadening in the ν_2 bands of HDO, $H_2^{16}O$, and $H_2^{18}O$. J Mol Spectrosc 1986;117:403–7.

[62] Adiks TG, Vinogradova AA, Malkov IP. Measurement of the absorption line parameters of water vapor in the 5.8 μm region using a tunable laser diode spectrometer. J Appl Spectrosc 1986;45:778–81.

[63] Hartmann JM, Taine J, Bonamy J, Labani B, Robert D. Collisional broadening of rotation–vibration lines for asymmetric-top molecules. II. H_2O diode laser measurements in the 400–900 K range; calculations in the 300–2000 K range. J Chem Phys 1987;86:144–56.

[64] Bauer A, Godon M, Kheddar M, Hartmann JM, Bonamy J, Robert D. Temperature and perturber dependences of water–vapor 380 GHz-line broadening. JQSRT 1987;37:531–9.

[65] Gasster SD, Townes CH, Goorvitch D, Valero FPJ. Foreign-gas collision broadening of the far-infrared spectrum of water vapor. JOSA B 1988;5:593–601.

[66] Bauer A, Godon M, Kheddar M, Hartmann JM. Temperature and perturber dependences of water vapor line-broadening. Experiments at 183 GHz; calculations below 1000 GHz. JQSRT 1989;41:49–54.

[67] Mandin JY, Chevillard JP, Flaud JM, Camy-Peyret C. N_2-broadening coefficients of $H_2^{16}O$ lines between 13500 and 19900 cm^{-1}. J Mol Spectrosc 1989;138:430–9.
[68] Goyette TM, De Lucia FC. The pressure broadening of the 3,1,3-2,2,0 transition of water between 80 and 600 K. J Mol Spectrosc 1990;143:346–58.
[69] Nicolaisen FM, 1990 ASA workshop paper 5.8, Moscow June 6–8, 1990.
[70] Aushev AF, Borisova NF, Bykova ES, Osipov VM, Tsukanov VV. On the temperature dependence of the half-widths of the spectral lines of CO_2 and H_2O. Opt Spectrosc 1990;68:700–1.
[71] Aggev BG, Ponomarev YuN, Tikhomirov BA, Tyryshkin IS. 1990 ASA workshop paper 5.9, Moscow June 6–8, 1990.
[72] Remedios JJ. PhD dissertation. University of Oxford, 1990.
[73] Rinsland CP, Goldman A, Smith MAH, Malathy Devi V. Measurements of Lorentz air-broadening coefficients and relative intensities in the $H_2^{16}O$ pure rotational and ν_2 bands from long horizontal path atmospheric spectra. Appl Opt 1991;30:1427–38.
[74] Arroyo MP, Hanson RK. 30th Aerospace Sciences Meetings & Exhibits paper AIAA 92-510, Reno Jan. 6–9, 1992.
[75] Malathy Devi V, Benner DC, Smith MAH, Rinsland CP. Measurements of pressure broadening and pressure shifting by nitrogen in the ν_1 and ν_3 bands of $H_2^{16}O$. J Mol Spectrosc 1992;155:333–42.
[76] Giesen T, Schieder R, Winnewisser G, Yamada KMT. Precise measurements of pressure broadening and shift for several H_2O lines in the ν_2 band by argon, nitrogen, oxygen, and air. J Mol Spectrosc 1992;153:406–18.
[77] Adler-Golden S, Lee J, Goldstein N. Diode laser measurements of temperature dependent line parameters for water vapor near 820 nm. JQSRT 1992;48:527–35.
[78] Avetisov VG, Nadezhdinskii AI, Khusnutdinov AN, Omarova PM, Zyrianov MV. Diode laser spectroscopy of water vapor in 1.8 μm: line profile measurements. J Mol Spectrosc 1993;160:326–34.
[79] Goyette TM, De Lucia FC, Dutta JM, Jones CR. Variable temperature pressure broadening of the $4_{1,4}$-$3_{2,1}$ transition of H_2O by O_2 and N_2. JQSRT 1993;49:485–9.
[80] Yamada KMT, Harter M, Giesen T. Survey study of air-broadened water vapor lines in the ν_2 band by high-resolution FTIR spectroscopy. J Mol Spectrosc 1993;157:84–94.
[81] Chu Z, Wilkerson TD, Singh UN. Water–vapor absorption line measurements in the 940-nm band by using a Raman-shifted dye laser. Appl Opt 1993;32:992–8.
[82] Mandin JY, Dana V, Badaoui M, Barbe A, Hamdouni A, Plateaux JJ. Measurements of pressure-broadening and pressure-shifting coefficients from FT spectra. J Mol Spectrosc 1994;164:328–37.
[83] Langlois S, Birbeck TP, Hanson RK. Temperature dependent collision broadening parameters of H_2O lines in the 1.4 μm region using diode laser absorption spectroscopy. J Mol Spectrosc 1994;167:272–81.
[84] Nagali V, Chou SI, Baer DS, Hanson RK. Diode laser measurements of temperature dependent half-widths of H_2O transitions in the 1.4 μm region. JQSRT 1997;57:795–809.
[85] Ponsardin PL, Browell EV. Measurements of $H_2^{16}O$ linestrengths and air-induced broadenings and shifts in the 815-nm spectral region. J Mol Spectrosc 1997;185:58–70.
[86] Schmucker N, Trojan Ch, Giesen T, Schieder R, Yamada KMT, Winnewisser G. Pressure broadening and shift of some H_2O lines in the ν_2 band: revisited. J Mol Spectrosc 1997;184:250–6.
[87] Chance KV, Park K, Evenson KM. Pressure broadening of far infrared rotational transitions: 88.65 cm^{-1} H_2O and 114.47 cm^{-1} O_3. JQSRT 1998;59:687–8.
[88] Gao-Junyi, Chen-Hongbing, Zhou-Jingang, Ma-Zhijun, Gong-Zhiben. Chinese J Quantum Electron 1998;15:186–92.
[89] Valentin A, Rachet C, Bykov AD, Lavrentieva NN, Saveliev VN, Sinitsa LN. J dependence of the Lineshift coefficients in the ν_2 water vapor band. JQSRT 1998;59:165–70.
[90] Valentin A, Claveau C, Bykov AD, Lavrentieva NN, Saveliev VN, Sinitsa LN. The water–vapor ν_2 band lineshift coefficients induced by nitrogen pressure. J Mol Spectrosc 1999;198:218–29.
[91] Davis SJ, Kessler WJ, Bachmann M. Collisional broadening of absorption lines in water vapor and atomic iodine relevant to COIL diagnostics. Proc SPIE, the Int Soc Opt Eng 1999;3612:157–66.
[92] Toth RA. Air- and N_2-broadening parameters of water vapor: 604 to 2271 cm^{-1}. J Mol Spectrosc 2000;201:218–43.
[93] Lucchesini A, Gozzini S, Gabbanini C. Water vapor overtones pressure broadening and shifting measurements. Eur Phys J 2000;D8:223–6.

[94] Claveau C, Henry A, Hurtmans D, Valentin A. Narrowing and broadening parameters of H_2O lines perturbed by He, Ne, Ar, Kr and nitrogen in the spectral range 1850–2140 cm^{-1}. JQSRT 2001;68:273–98.

[95] Schermaul R, Learner RCM, Newnham DA, Williams RG, Ballard J, Zobov NF, Belmiloud D, Tennyson J. The water vapor spectrum in the region 8600–15000 cm^{-1}: experimental and theoretical studies to a new spectral line database. J Mol Spectrosc 2001;208:32–42.

[96] Lepère M, Henry A, Valentin A, Camy-Peyret C. Diode-laser spectroscopy: line profiles of H_2O in the region of 1.39 μm. J Mol Spectrosc 2001;208:25–31.

[97] Moretti L, Sasso A, Gianfrani L, Ciurylo R. Collisional-broadened and Dicke-narrowed lineshapes of $H_2^{16}O$ and $H_2^{18}O$ transitions at 1.39 μm. J Mol Spectrosc 2001;205:20–7.

[98] Steyert DW, Wang WF, Sirota JM, Donahue NM, Reuter DC. Pressure broadening coefficients for rotational transitions of water in the 380–600 cm^{-1} range. JQSRT 2002;72:775–82.

[99] Coheur PF, Fally S, Carleer M, Clerbaux C, Colin R, Jenouvrier A, Mérienne MF, Hermans C, Vandaele AC. New water vapor line parameters in the 26000–13000 cm^{-1} region. JQSRT 2002;74:493–510.

[100] Claveau C, Henry A, Lepère M, Valentin A, Hurtmans D. Narrowing and broadening parameters for H_2O lines in the ν_2 band perturbed by nitrogen from Fourier transform and tunable diode laser spectroscopy. J Mol Spectrosc, in press.

[101] Brown L. Line broadening and shifting of transitions in the 1 μm region. Private communication.

[102] Newnham DA. Line broadening and shifting of transitions in the region of the ν_2 band. Private communication.

[103] Bonamy J, Robert D, Boulet C. Simplified models for the temperature dependence of linewidths at elevated temperature and application to CO broadened by ar and N_2. JQSRT 1984;31:23–34.

[104] Watson JKG. Determination of centrifugal distortion coefficients of asymmetric-top molecules. J Chem Phys 1967;46:1935–49.

[105] Matsushima F, Odashima H, Iwaskai T, Tsunekawa S. Frequency measurement of pure rotational transitions of H_2O from 0.5 to 5 THz. J Mol Struct 1995;352–353:371–8.

[106] Flaud JM, C. Camy-Peyret C. Watson Hamiltonian constants for the first vibrational levels of H_2O. Private communication.

[107] Grossmann BE, Browell EV, Bykov AD, Kapitanov VA, Lazarev VV, Ponomarev YN, Sinitsa LN, Korotchenko Ea, Stroinova VN, Tikhomirov BA. Investigation of H_2O absorption line shifts caused by air pressure in the visible. Atm Opt 1990;3:617–29.

[108] Huber KP, Herzberg G. Molecular spectra and molecular structure constants of diatomic molecules. New York: Van Nostrand, 1979.

[109] Shostak SL, Muenter JS. The dipole moment of water. II. Analysis of the vibrational dependence of the dipole moment in terms of a dipole moment function. J Chem Phys 1991;94:5883–90.

[110] Flygare WH, Benson RC. Molecular Zeeman effect in diamagnetic molecules and the determination of molecular magnetic moments (g values), magnetic susceptibilities, and molecular quadrupole moments. Mol Phys 1971;20:225–50.

[111] Mulder F, Van Dijk G, Van der Avoird A. Multipole moments, polarizabilities, and anisotropic long range interaction coefficients for nitrogen. Mol Phys 1980;39:407–25.

[112] Lide DR, editor. CRC handbook of physics and chemistry, 77th ed. Cleavland, OH: The Chemical Rubber Company, 1996.

[113] Bogaard MP, Orr BJ. MPT international review of science. In: Buckingham AD, editor, Physical chemistry, series two, vol. 2, Molecular structure and properties. London: Butterworths, 1975 [Chapter 5].

[114] Lofthus A. The molecular spectrum of nitrogen. Department of Physics, University of Oslo, Blindern, Norway, Spectroscopic Report No. 2, 1, 1960.

[115] Bouanich JP. Site-site Lennard-Jones potential parameters for nitrogen, oxygen, hydrogen, carbon monoxide and carbon dioxide. JQSRT 1992;47:243–50.

[116] Gamache RR, Fischer J. Half-widths of $H_2^{16}O$, $H_2^{18}O$, $H_2^{17}O$, $HD^{16}O$, and $D_2^{16}O$: II Comparison with measurements. JQSRT, submitted for publications.

[117] Diaz Pena M, Pando C, Renuncio JAR. Combination rules for intermolecular potential parameters. I. Rules based on approximations for the long-range dispersion energy. J Chem Phys 1982;76:325–32.

[118] Diaz Pena M, Pando C, Renuncio JAR. Combination rules for intermolecular potential parameters. I. Rules based on approximations for the long-range dispersion energy and an atomic distortion model for the repulsive interactions. J Chem Phys 1982;76:333–9.

[119] Gamache RR, Rosenmann L. The effects of velocity averaging in broadening coefficient calculations. J Mol Spectrosc 1994;164:489–99.

[120] Pickett HM. Effects of velocity averaging on the shapes of absorption lines. J Chem Phys 1980;73:6090–4.

[121] Lance B, Robert D. An analytical model for collisional effects on spectral line shape from the Doppler to the collision regime. J Chem Phys 1998;109:8283–8.

[122] Mandin JY, Flaud JM, Camy–Peyret C. Measurements and calculations of self-broadening coefficients of lines belonging to the v_2 band of $H_2^{16}O$. JQSRT 1980;23:351–70.